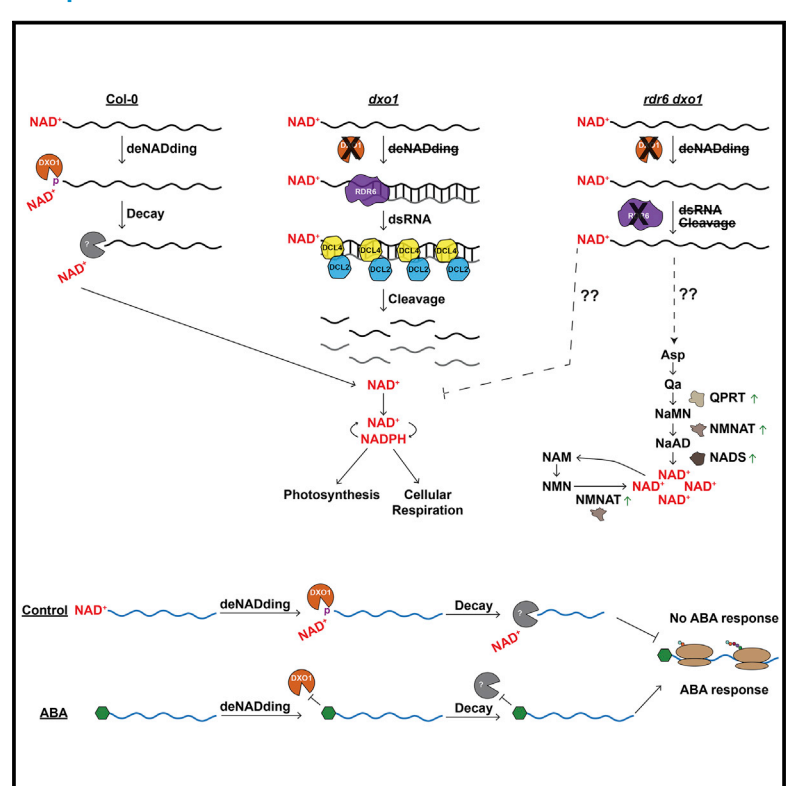


Messenger RNA 5' NAD⁺ Capping Is a Dynamic Regulatory Epitranscriptome Mark That Is Required for Proper Response to Abscisic Acid in Arabidopsis

Graphical Abstract



Authors

Xiang Yu, Matthew R. Willmann, Lee E. Vandivier, ..., Eric Lyons, Nathaniel W. Snyder, Brian D. Gregory

Correspondence

bdgregor@sas.upenn.edu

In Brief

Eukaryotic RNAs have been found to contain 5'-end NAD+ caps, but the dynamic nature of these modifications is unknown. Yu et al. demonstrate that plant response to the phytohormone abscisic acid (ABA) reshapes RNA NAD+ capping to stabilize transcripts encoding ABA response proteins, allowing proper response to this essential phytohormone.

Highlights

- Messenger RNA NAD⁺ capping is widespread and varies between tissues in plants
- NAD⁺-capped RNAs are unstable and a lack of their turnover induces NAD⁺ metabolism
- Plant response to abscisic acid (ABA) remodels the NAD⁺-capped transcriptome
- Much of the ABA-mediated NAD⁺ transcriptome reprogramming does not require DXO1







Article

Messenger RNA 5' NAD⁺ Capping Is a Dynamic Regulatory Epitranscriptome Mark That Is Required for Proper Response to Abscisic Acid in Arabidopsis

Xiang Yu,¹ Matthew R. Willmann,² Lee E. Vandivier,^{1,3} Sophie Trefely,^{4,5,6} Marianne C. Kramer,^{1,3} Jeffrey Shapiro,¹ Rong Guo,¹ Eric Lyons,^{7,8} Nathaniel W. Snyder,⁶ and Brian D. Gregory^{1,3,9,*}

SUMMARY

Although eukaryotic messenger RNAs (mRNAs) normally possess a 5′ end N⁷-methyl guanosine (m⁷G) cap, a non-canonical 5′ nicotinamide adenine dinucleotide (NAD⁺) cap can tag certain transcripts for degradation mediated by the NAD⁺ decapping enzyme DXO1. Despite this importance, whether NAD⁺ capping dynamically responds to specific stimuli to regulate eukaryotic transcriptomes remains unknown. Here, we reveal a link between NAD⁺ capping and tissue- and hormone response-specific mRNA stability. In the absence of DXO1 function, transcripts displaying a high proportion of NAD⁺ capping are instead processed into RNA-dependent RNA polymerase 6-dependent small RNAs, resulting in their continued turnover likely to free the NAD⁺ molecules. Additionally, the NAD⁺-capped transcriptome is significantly remodeled in response to the essential plant hormone abscisic acid in a mechanism that is primarily independent of DXO1. Overall, our findings reveal a previously uncharacterized and essential role of NAD⁺ capping in dynamically regulating transcript stability during specific physiological responses.

INTRODUCTION

The 5′ end of eukaryotic mRNAs is co-transcriptionally modified through the addition of a 7-methylguanosine cap (m⁷G), which functions through interaction with various cap-binding proteins to protect mature mRNAs from degradation by 5′ to 3′ exonucleases (Zhang and Guo, 2017). The m⁷G additionally acts as a unique identifier to regulate nuclear export, polyadenylation, pre-mRNA splicing, and promotes translation initiation of mature mRNAs (Gonatopoulos-Pournatzis and Cowling, 2014). Thus, removal of the cap along with the 3′ end polyadenine (polyA) tail are both critical steps for regulating mRNA degradation in eukaryotes. DECAPPING2 (DCP2) is the well-known m⁷G decapping enzyme (Valkov et al., 2016), but eukaryotic genomes encode other enzymes with decapping activity, and much less is known about the functional relevance of these proteins.

Recently, a different type of 5' cap structure, a nicotinamide adenine dinucleotide (NAD⁺) cap has been identified on bacterial RNAs (Chen et al., 2009; Cahová et al., 2015; Bird et al., 2016;

Vvedenskaya et al., 2018; Frindert et al., 2018), yeast RNAs (Walters et al, 2017), mammalian RNAs (Jiao et al., 2017; Bird et al., 2018), and plant RNAs (Wang et al., 2019; Zhang et al., 2019; Kwasnik et al., 2019; Pan et al., 2020). In contrast to the m⁷G cap, the NAD⁺ cap promotes degradation of specific transcripts, revealing it as a potential 5' cap-mediated epitranscriptomic regulator. More specifically, the resulting NAD⁺-capped mRNAs are eventually decapped and degraded by the enzyme Rai1/ DXO1 (hereafter DXO1) (Jiao et al., 2017).

DXO1 has dual functions, as it can remove the NAD⁺ cap through a process called "deNADding" as well as degrade and clear these non-canonically capped transcripts (Xiang et al., 2009; Chang et al., 2012; Jiao et al., 2017). In mammalian cells, DXO1 removes this moiety from NAD⁺-capped transcripts, resulting in free NAD⁺ molecules and 5' mono-phosphorylated (5' P) transcripts, and subsequently degrades the resulting 5' P mRNA via its 5'–3' exoribonuclease activity (Jiao et al., 2017; Kiledjian, 2018). In the model plant *Arabidopsis thaliana* (hereafter Arabidopsis), the DXO1 ortholog possesses NAD⁺ decapping

¹Department of Biology, University of Pennsylvania, Philadelphia, PA 19104, USA

²School of Integrative Plant Science, Cornell University, Ithaca, NY 14853, USA

³Cell and Molecular Biology Graduate Group, Perelman School of Medicine, University of Pennsylvania, Philadelphia, PA 19104, USA

⁴Department of Cancer Biology, Perelman School of Medicine, University of Pennsylvania, Philadelphia, PA 19104, USA

⁵Abramson Family Cancer Research Institute, Perelman School of Medicine, University of Pennsylvania, Philadelphia, PA 19104, USA

⁶Center for Metabolic Disease Research, Department of Microbiology and Immunology, Lewis Katz School of Medicine, Temple University, Philadelphia, PA 19140, USA

⁷School of Plant Sciences, University of Arizona, Tucson, AZ 85721, USA

⁸CyVerse, University of Arizona, Tucson, AZ 85721, USA

⁹Lead Contact

^{*}Correspondence: bdgregor@sas.upenn.edu https://doi.org/10.1016/j.devcel.2020.11.009





activity in vitro (Kwasnik et al., 2019; Pan et al., 2020), suggesting that DXO1 is a major regulator of NAD+-capped transcripts in mammals and plants. While it is evident that NAD+ decapping and subsequent RNA removal can regulate mRNA abundance, the physiological relevance of this turnover and whether NAD+ capping could be a mechanism for dynamic regulation of mRNA stability in response to cellular signals are completely unstudied.

RNA degradation directed by small non-coding RNAs (smRNAs) is an additional RNA turnover mechanism to precisely control mRNA abundance post-transcriptionally. In one such plant pathway, 21-22 nucleotide (nt) smRNAs are generated by DCL cleavage of double-stranded RNAs produced by RNAdependent RNA polymerase 6 (RDR6) (Willmann et al., 2011). This post-transcriptional gene silencing (PTGS) pathway can be triggered as a secondary control mechanism by exogenous RNAs when canonical RNA surveillance pathways are absent and/or normal RNA processing is impaired (Baulcombe, 1996; Liu and Chen, 2016). In fact, losing the function of DCP2, capbinding proteins (e.g., CBP80/ABH1) or EXORIBONUCLEASE 4 (XRN4) can induce these PTGS pathways (Gregory et al., 2008; Martínez de Alba et al., 2015; Zhang et al., 2015), suggesting they are backup mechanisms to tightly control mRNA abundance. Recently, it was also demonstrated that loss of DXO1 function resulted in PTGS-mediated smRNA processing from over 1,000 protein-coding mRNAs in Arabidopsis (Kwasnik et al., 2019; Pan et al., 2020). However, the significance of this smRNA processing is unclear, since their presence does not contribute to developmental defects of dxo1 mutant plants (Kwasnik et al., 2019; Pan et al., 2020).

Abscisic acid (ABA) is a major plant hormone that is involved in responses to many environmental stresses and controls the transition of seeds from dormancy to germination (Finkelstein, 2013). In fact, impairment of m⁷G cap recognition and decapping, as well as RNA degradation, alter plant sensitivity to ABA and abiotic stresses by regulating the biosynthesis, signal transduction, and expression of downstream ABA-responsive genes (Hugouvieux et al., 2001; Wawer et al., 2018). While the importance of regulating removal of the canonical m⁷G cap in ABA response is evident, whether decapping of the non-canonical 5' NAD+ cap is important for response to ABA has not been explored.

Here, we use a variant of NAD-capture sequencing (Cahová et al., 2015) in combination with degradome and RNA sequencing (RNA-seq) to identify NAD+-capped RNAs in Arabidopsis unopened flower buds, and during seedling response to the phytohormone ABA, and examine the role of this moiety in regulating mRNA stability. This analysis reveals that RNA NAD+ capping is widespread and varies between plant tissues to destabilize specific subsets of the transcriptome when they are not required. Our findings also illuminate a previously uncharacterized mechanism in which mRNA NAD+ caps can be dynamically regulated to affect a eukaryotic physiological response.

RESULTS

DXO1 Acts as an Eraser of RNA 5' End NAD+ Caps in **Arabidopsis**

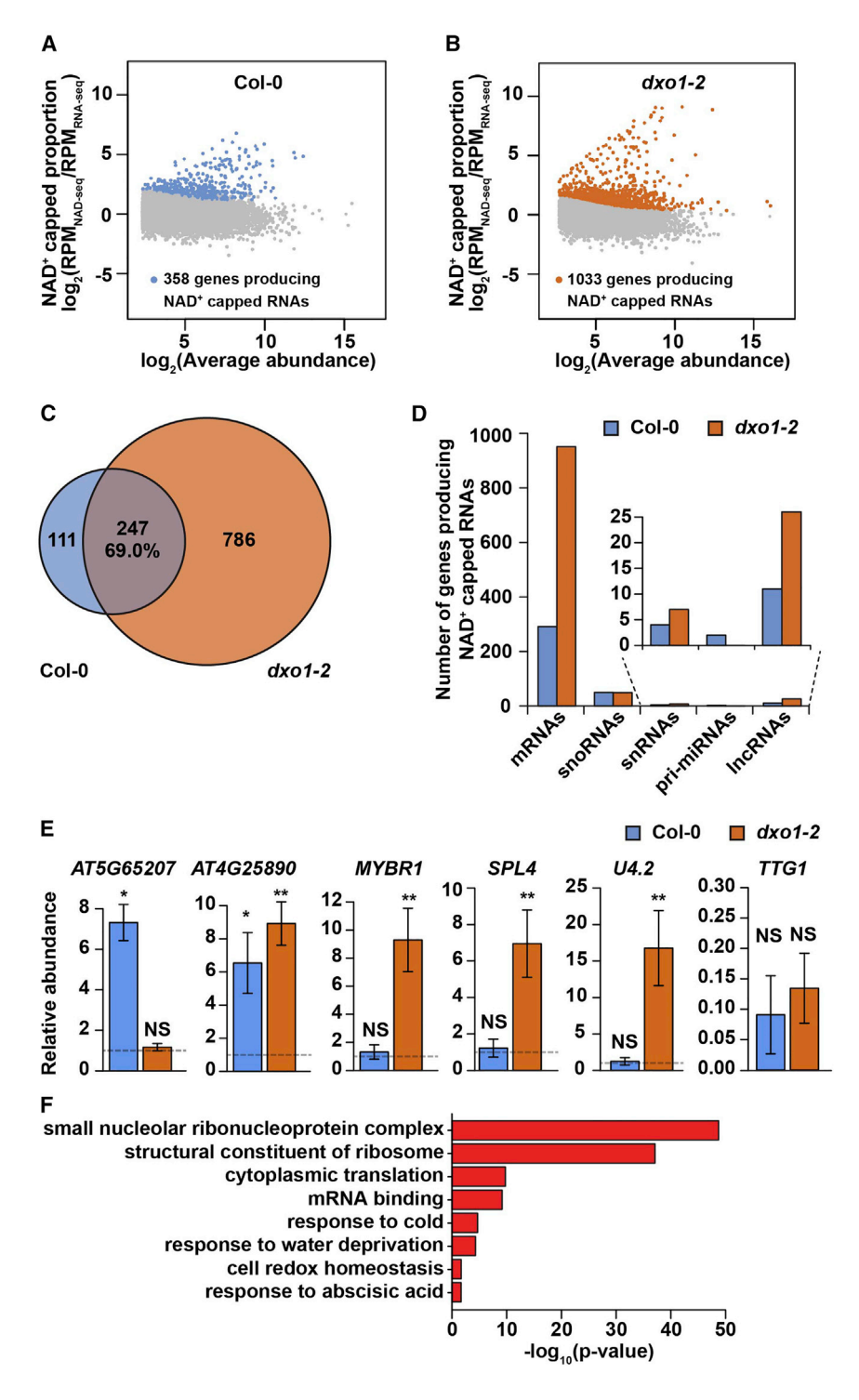
AtDXO1 (AT4G17620) is the single copy Arabidopsis ortholog of mammalian DXO1 (Figure S1A). According to available data (Klepikova et al., 2016), the DXO1 transcript is highly abundant in roots, young leaves, inflorescence shoot apex, flower buds, and dry seeds, suggesting the importance of DXO1 to Arabidopsis development (Figure S1B). To test this, we obtained two independent DXO1 mutant alleles, dxo1-1 and dxo1-2 (Figure S1C). Supporting our hypothesis and previous findings (Kwasnik et al., 2019; Pan et al., 2020), both dxo1 mutant alleles display severe developmental defects as compared with wild-type Columbia-0 (hereafter Col-0) plants. In fact, 2-week-old dxo1 mutant seedlings showed dwarfism and yellow coloration (Figure S1D), 3-week-old dxo1 plants displayed growth delays as measured by a decrease in leaf number (Figure S1E), and flowering dxo1 mutant plants were significantly less fertile with much shorter siliques (Figure S1F). Arabidopsis transgenic lines expressing the fusion protein of DXO1 and β-glucuronidase (GUS) in the dxo1-2 mutant background rescued the mutant phenotype, indicating that loss of DXO1 results in the aberrant phenotypes observed (Figure S1G). Additionally, GUS staining revealed that DXO1 is highly abundant in shoot and root apices (Figure S1H). To determine the subcellular localization of DXO1, we generated transgenic lines in the dxo1-2 mutant background expressing eGFP-tagged DXO1 and found that DXO1 is localized to both the nucleus and cytoplasm in protoplasts and root tips (Figures S1I and S1J). These results reveal that DXO1 is localized throughout the cell and plays critical functions in both vegetative and reproductive developmental processes, displaying its importance to plant biology.

While previous studies demonstrated that DXO1 functions in the decapping of RNA 5' end NAD+ caps in vitro (Kwasnik et al., 2019), whether it has the same function in vivo is unknown. To test this, we performed NAD-capture sequencing with the slight variation that full NAD+-capped transcripts were used as the substrate in RNA sequencing library preparation (hereafter NAD-seq) (Cahová et al., 2015; Zheng et al., 2010; Li et al., 2012; Figure S2A). To begin, we validated the NAD+ capture approach using in vitro synthesized luciferase (LUC) transcripts with and without the addition of a NAD+ cap followed by RTqPCR. As expected, we captured only NAD+ modified LUC transcripts after ADP-ribosylcyclase (ADPRC) treatment compared with unmodified LUC transcripts (Figure S2B). With this proof of principle, we performed NAD-seq in two biological replicates of Col-0 and dxo1-2 mutant unopened flower buds (Figures S1B and S1F). In tandem, we performed total RNA-seq for these same samples to serve as a background for identifying NAD+capped transcripts. The resulting NAD-seq and RNA-seq libraries were sequenced and provided ~11-20 million mapped reads per library. The biological replicates of each library type from the distinct genotypes clustered together (Figures S2C and S2D), indicating the high quality and reproducibility of these

Similar to studies in mammalian cells (Jiao et al., 2017), we found a significant (p value < 0.001, Chi-squared test) increase in the ratio of reads uniquely mapping to mRNAs as compared with rRNAs in dxo1-2 mutants compared with Col-0 libraries (Figure S2E), indicating that NAD+-capped mRNAs were enriched in the absence of DXO1 function. Using these datasets, we calculated the NAD+-capped proportion (log₂[RPM_{NAD-seq}/ RPM_{RNA-seq}]) for each transcript in Col-0 and dxo1-2 mutants, and found a significantly (p value < 0.001, Mann-Whitney U

Article





test) increased level of proportion NAD+ capping in the transcriptome of dxo1 mutant as compared with Col-0 (Figure S2F), indicating that DXO1 is also a plant deNADding enzyme. Using this statistic, we were also able to identify 358 and 1,033 genes producing significantly (FDR < 0.1, DESeq2) high proportion NAD+capped values in Col-0 and dxo1-2 unopened flower buds, respectively (Figures 1A and 1B; Tables S1 and S2). Most of the genes producing NAD+-capped transcripts (hereafter also

Figure 1. NAD-Seq Reveals that DXO1 Functions as a deNADding Enzyme In Planta (A and B) MA plots showing genes producing NAD+-capped RNAs enriched in Col-0 (A) (blue) and dxo1-2 mutant (B) (orange) unopened flower

(C) The overlap of genes producing NAD+-capped RNAs identified in Col-0 (blue) and dxo1-2 mutant (orange) unopened flower buds.

(D) The number of genes producing NAD+-capped RNAs encoding mRNAs, snoRNAs, snRNAs, primiRNAs, and IncRNAs in Col-0 (blue bars) and dxo1-2 mutant (orange bars) unopened flower

(E) The relative abundance of AT5G65207, AT4G25890, MYBR1, SPL4, U4.2, and TTG1 in NAD+-captured RNA samples as compared to total RNA samples containing in vitro transcribed NAD+ LUC as a spike-in control. The dashed lines indicate the average abundance of the indicated transcripts in total RNA samples normalized to NAD+ LUC as a spike-in control. NS denotes no significance, while * and ** denote p value < 0.05 and 0.01, respectively, Student's t test.

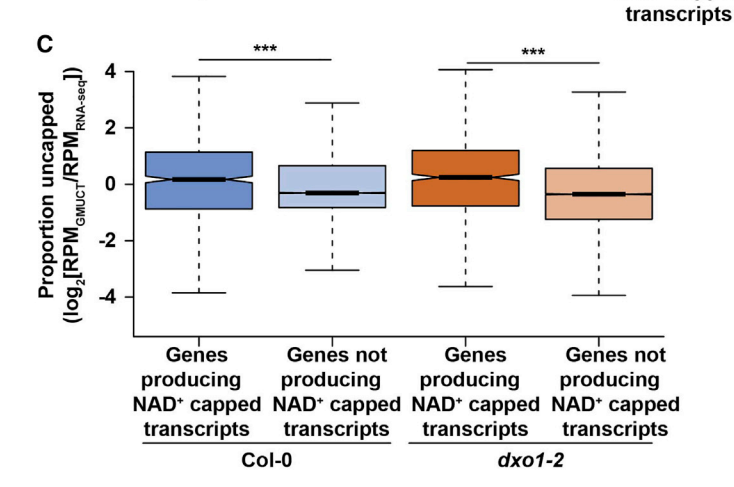
Error bars indicate ± standard error of the mean. (F) The enriched GO terms for 1,033 DXO1 de-NADding targets ordered by $-\log_{10}(p \text{ value})$.

referred to as NAD+-capped transcripts) identified in Col-0 (247; 69%) were also identified in the dxo1-2 plants, while an additional 786 were found only in the absence of DXO1 function (Figure 1C). These 786 NAD+-capped transcripts were likely not detected in Col-0 because their NAD+ cap was efficiently removed by DXO1. In agreement with prior data (Jiao et al., 2017), the majority of NAD+-capped transcripts identified in the dxo1-2 mutant, and thus, dependent on DXO1 function for their deNADding, are protein-coding mRNAs (951; 92.1%) and small nucleolar RNAs (snoRNAs; 49; 4.7%) (Figure 1D; Table S1). We also identified 26 long non-coding RNAs (IncRNAs) and seven small nuclear RNAs (snRNAs) with NAD+ caps, indicating that NAD+ caps can be added to a variety of transcripts (Figure 1D). To validate these results, we performed NAD capture followed by quantitative PCR for five randomly selected NAD+-capped transcripts (one NAD+-capped only in Col-

0 (AT5G65207), one modified in both genotypes (AT4G25890), and three NAD+-capped only in dxo1 mutants (MYBR1, SPL4, and U4.2)), as well as a non-NAD⁺-capped transcript in either genotype (TTG1). We included a NAD+-capped LUC as an RNA spike-in control. Consistent with our NAD-seg results, we found that SPL4, MYBR1, and U4.2 produced significantly (p values < 0.01, Student's t test) enriched pools of NAD+-capped transcripts compared with total RNAs containing the NAD+ LUC



В NS Change in RNA abundance Change in RNA abundance 10 (log₂[RPM_{dxo}/RPM_{col-0}]) (log₂[RPM_{dxo}/RPM_{col-0}]) 1.0 5 0.5 0.0 -0.5 -1.0 Differentially abundant transcripts -10 Genes producing NAD+ capped RNAs Genes



10

log₂(Average abundance)

15

spike-in control specifically in dxo1-2 mutant plants. In further support of the NAD-seq findings, AT5G65207 and AT4G25890 displayed NAD+-capped transcript enrichment (p value < 0.05, Student's t test) specifically in Col-0 and both genotypes. respectively (Figure 1E), while the negative control TTG1 displayed no enrichment in either genotype (relative abundance < 0) (Figure 1E). Overall, our NAD-seq results reveal that DXO1 functions in vivo as a deNADding enzyme that primarily targets protein-coding mRNAs but can also remove this modification from various non-coding RNAs.

We performed gene ontology (GO) enrichment analysis using the database for annotation, visualization, and integrated data (DAVID) (Huang et al., 2009) on the 1,033 DXO1 deNADding targets to characterize the biological processes that were likely regulated by NAD+ capping (Figures 1B-1D). NAD+-capped transcripts were enriched for those encoding proteins involved in cytoplasmic translation and mRNA binding, as well as numerous abiotic stress responses, including response to cold, water deprivation, and ABA (Figure 1F). They were also highly enriched for mRNAs encoding proteins involved in cell redox homeostasis (Figure 1F), a process where free NAD+ is an essential cofactor for redox coupling in all living cells (Xiao et al., 2018). Using the MapMan tool (Thimm et al., 2004), we took a closer look at what transcripts are NAD+-capped in this GO term and found that those in this functional class encode thioredoxin proteins, one class of redox proteins (Figure S2G). Thus, there may be a feedback mechanism wherein NAD+ caps tag transcripts encoding redox

Developmental Cell

Figure 2. DXO1 Functions in NAD+ Decapping-Directed RNA Turnover

(A) MA plot showing differentially abundant transcripts (pink, FDR < 0.05) between Col-0 and dxo1 mutant unopened flower buds. Red indicates genes producing NAD+-capped mRNAs in dxo1 plants (N = 951).

(B) The fold change of RNA abundance (log₂[RPM_{dxo1}/RPM_{Col-0}]) for genes producing NAD+-capped mRNAs (N = 951) and those without a NAD+ cap (N = 26,465). NS denotes no significance, Mann-Whitney U test.

(C) The proportion uncapped value of genes producing transcripts with a NAD+ cap and those without a NAD+ cap in Col-0 (dark and light blue, respectively) and dxo1 mutant (dark and light orange, respectively) plants. *** denotes p value < 0.001, Mann-Whitney U test.

Genes not

producing

transcripts

NAD* capped NAD* capped

producing

proteins functioning in reducing or oxidizing NAD+/NADH for post-transcriptional regulation. In total, our findings reveal that DXO1 is an in vivo NAD+ decapping enzyme, and this modification is added to a specific set of transcripts in plant unopened flower buds.

Arabidopsis DXO1 Functions in deNADding-Mediated RNA **Turnover**

We investigated the transcriptome changes that occur in the absence of

DXO1 function. To do this, we performed polyA+ RNA sequencing (mRNA-seq) in unopened flower buds from two biological replicates of Col-0 and one biological replicate for each dxo1 mutant allele to act as biological replicates of each other given their similar phenotypes, which produced ~11-19 million mapped reads per library. The biological replicates from the both dxo1 mutant alleles clustered together and were distinct from those for Col-0 (Figure S3A), indicating the high quality and reproducibility of these libraries. Using edgeR (Robinson et al., 2010), we identified 1,230 and 1,506 transcripts that were significantly more and less abundant, respectively, in the dxo1 mutant as compared with Col-0 plants (Figure 2A). To determine if the transcript abundance for NAD+-capped RNAs changed in the absence of DXO1, we focused on the 951 protein-coding transcripts that are dependent on DXO1 for their decapping (Figure 1C). The abundance of these transcript populations did not significantly change in dxo1 mutants compared with Col-0 (Figures 2A and 2B), nor was the RNA abundance for NAD+-capped transcripts significantly different than those not producing these modified RNAs (Figure 2B). Thus, the presence of a NAD+ cap does not affect their overall level of abundance in the dxo1 mutant plants (Figure 2A), suggesting additional posttranscriptional control of these RNAs.

To determine if NAD+ capping affects transcript stability, we performed genome-wide mapping of uncapped and cleaved transcripts (GMUCT) (Gregory et al., 2008; Willmann et al., 2014) to quantify the degradation and cleaved intermediates of

Article



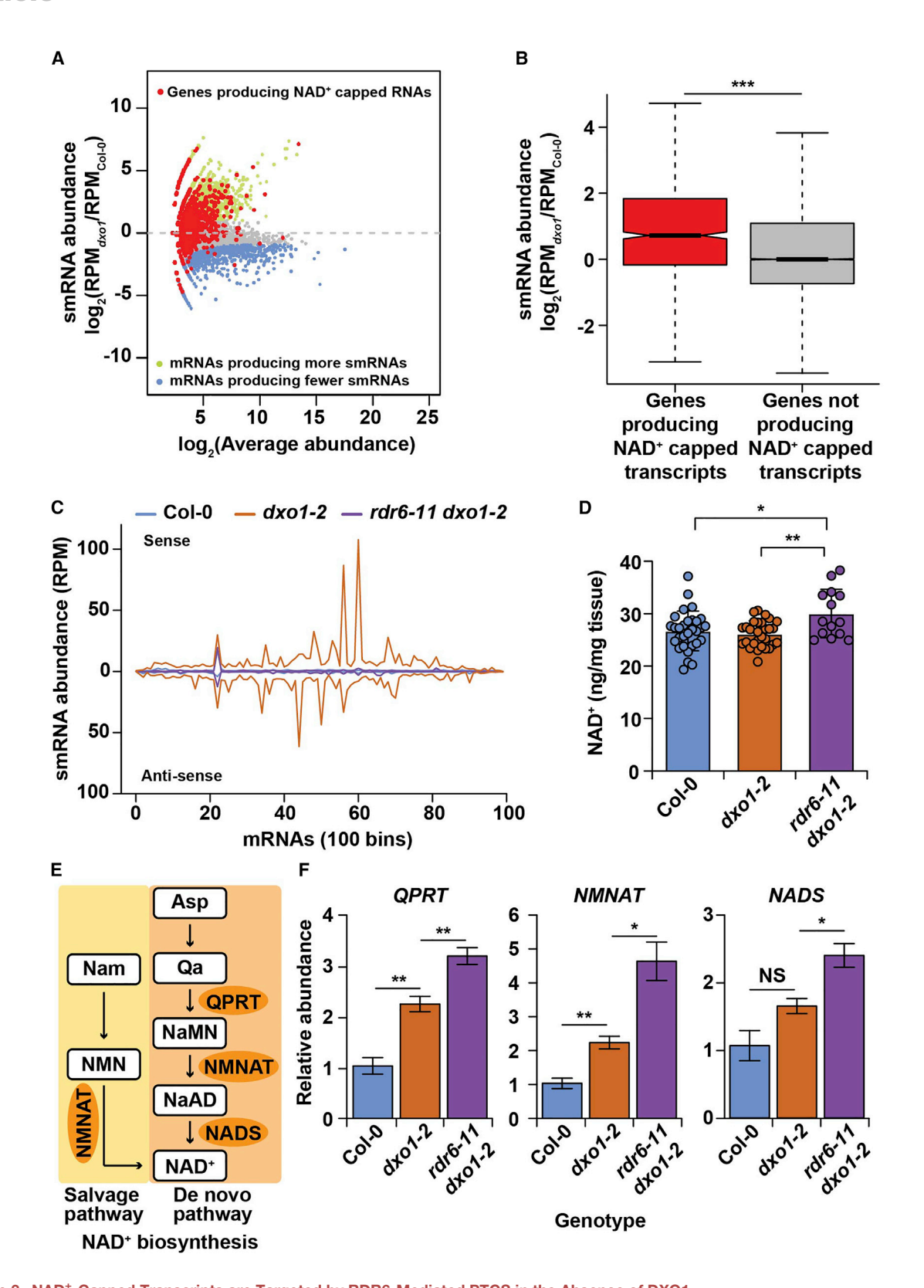


Figure 3. NAD*-Capped Transcripts are Targeted by RDR6-Mediated PTGS in the Absence of DXO1

(A) MA plot showing mRNAs that produce significantly (adjusted p value < 0.05) more (green) and less (blue) smRNAs in *dxo1* mutants compared with Col-0. Red dots highlight mRNAs with a NAD* cap (N = 951).





polyA+ transcripts in the same samples used for mRNA-seq. The Col-0 GMUCT libraries have been previously analyzed and described (Willmann et al., 2014), while the resulting dxo1 mutant GMUCT libraries were sequenced and provided ~25 and 35 million mapped reads in the two libraries. The biological replicates from both dxo1 mutant alleles clustered together and were distinct from Col-0, indicating the high quality and reproducibility of the GMUCT libraries (Figure S3B). Using the GMUCT and mRNA-seq data, we measured the relative stability of transcripts using the proportion uncapped metric (log₂[RPM_{GMUCT}/ RPM_{RNA-seq}]) (Vandivier et al., 2015; Anderson et al., 2018), where a higher value correlates with a less stable transcript and vice versa.

We first compared the proportion uncapped for NAD+-capped transcripts to those that lack this modification in Col-0 and dxo1 mutant plants. As expected, we found that NAD+-capped transcripts display a significantly (p value < 0.001, Mann-Whitney U test) higher proportion of uncapped value (less stable) than those that lack this modification in Col-0, revealing that, similar to in mammals (Jiao et al., 2017), these RNAs tend to be unstable (Figure 2C). We also observed that the stability of these transcripts is unchanged in dxo1 mutants, as transcripts with a high proportion of NAD+ capping are significantly (p value < 0.001, Mann-Whitney U test) less stable than those without a NAD+ cap, and their proportion uncapped values were similar between Col-0 and dxo1 mutants (Figure 2C). This indicates that while DXO1 is required for decapping of these transcripts, there is an additional pathway for destabilizing of NAD+-capped transcripts when this enzyme is non-functional.

NAD*-Capped Transcripts Are Processed into Small **RNAs in the Absence of DXO1 Function**

Since we observed that NAD+-capped transcripts are unstable even in dxo1 mutant plants, it is likely that there is an additional mechanism to destabilize them when DXO1 function is absent. Prior studies revealed that an accumulation of transcripts with non-canonical 5' ends can trigger their processing into smRNAs through RDR6-dependent PTGS (Herr et al., 2006; Martínez de Alba et al., 2015; Gregory et al., 2008; Zhang et al., 2015). Thus, we hypothesized that the accumulation of NAD+-capped transcripts in dxo1 mutant plants (Figures 1B and 1C) could trigger degradation through PTGS. To test this, we performed small RNA sequencing (smRNA-seq) using the same samples as for mRNA-seq, which produced ~11-40 million mapped reads per library. The biological replicates from both dxo1 mutant alleles clustered together and were distinct from Col-0, indicating the high quality and reproducibility of the libraries (Figure S4A). We found that 21 and 22 nt smRNAs derived from both

strands of protein-coding transcripts accumulated in dxo1 mutant compared with Col-0 plants (Figures 3A and S4B-S4D).

In total, 2,337 and 1,282 mRNAs produced significantly (adjusted p value < 0.05, edgeR) more and less 21-22 nt smRNAs, respectively, in dxo1 mutants compared with Col-0 plants, (Figure 3A; Table S3). Additionally, we found that NAD+-capped transcripts in dxo1 mutant flower buds (Figure 1B) produced significantly (p value < 0.001, Mann-Whitney U test) more 21-22 nt smRNAs than those without NAD+ caps (Figures 3A and 3B). In fact, when the collection of NAD+-capped transcripts was separated into quartiles based on their increasing NAD+-capped proportion values (quartile 1 lowest and 4 highest), we observed significant (all p values < 0.05, Mann-Whitney U test) monotonic increases in the levels of smRNAs produced in dxo1 mutant compared with Col-0 flower buds. For example, two NAD+-capped transcripts, AT4G18670 and AT2G45470, accumulated significantly (p value < 0.001, Student's t test) higher levels of 21-22 nt smRNAs from both their sense and antisense strands in dxo1 mutant compared with Col-0 plants (Figures S4B and S4C), suggesting RDR6 is involved in their biogenesis. Our findings reveal that NAD+-capped transcripts are processed into smRNAs in the absence of DXO1 function (Figures 3A, 3B, and S4B-S4E), providing a mechanism to keep their levels of stability and total abundance similar to those in Col-0 plants (Figure 2).

As NAD+-capped transcripts appear to be targeted for RDR6-dependent PTGS in the absence of DXO1, we tested this by crossing a null mutation of RDR6 (rdr6-11) into the dxo1-2 mutant background, resulting in plants that have lost the function of both RDR6 and DXO1 simultaneously (rdr6-11 dxo1-2). We then tested if this PTGS pathway was responsible for the processing of smRNAs from NAD+-capped transcripts in the absence of DXO1 by performing smRNA-seq in unopened flower buds from the rdr6-11 dxo1-2 double mutants (Figure S4A). We found that smRNAs processed from these transcripts were reduced to levels similar to those in Col-0 in the rdr6-11 dxo1-2 double mutant plants (Figure 3C), indicating that RDR6 is required for the biogenesis of smRNAs from NAD+-capped transcripts in the absence of DXO1 mutant function. We also found that the impairment of RDR6 function did not rescue the morphological defects observed in dxo1 mutant plants, as dxo1 single and rdr6-11 dxo1-2 double mutant plants displayed identical phenotypes (Figure S4F), consistent with previous reports (Kwasnik et al., 2019; Pan et al., 2020). These findings suggest that plant cells might use smRNA biogenesis as an RNA degradation pathway for NAD+-capped transcripts in the absence of DXO1 function, but this hypothesis needs further exploration.

⁽B) Fold change of 21–22 nt smRNA abundance from DXO1-regulated mRNAs with NAD+ caps (N = 951) and mRNAs without NAD+ caps (N = 26,258) in dxo1 mutants as compared with Col-0. *** denotes p value < 0.001, Mann-Whitney U test.

⁽C) The distribution of 21–22 nt smRNAs along both strands of mRNAs with a significant proportion of NAD* capping in Col-0 (blue), dxo1 single (orange), and rdr6-11 dxo1-2 double mutant (purple) unopened flower buds. Signal above/below the 0 line indicates the reads (RPM) mapped to the sense/antisense strand of

⁽D) Quantification of total NAD+ levels in Col-0 (blue), dxo1-2 single (orange), and rdr6-11 dxo1-2 double mutant (purple) 21-day-old seedlings. Dots indicate individual biological replicates. Error bars indicate ± standard error of the mean.

⁽E) A schematic diagram illustrating the key steps of de novo (orange background) and salvage pathways (yellow background) for NAD⁺ biosynthesis in plants. (F) The relative abundance of transcripts encoding NAD+ biosynthesis proteins QPRT, NMNAT, and NADS in Col-0 (blue), dxo1-2 (orange), and rdr6-11 dxo1-2 (purple). The values are normalized to those for Col-0 and the ACT1 transcript as an internal control. Error bars indicate ± standard error of the mean. (D and F) NS denotes no significance. * and ** denote p value < 0.05 and 0.01, respectively, Student's t test.

Article



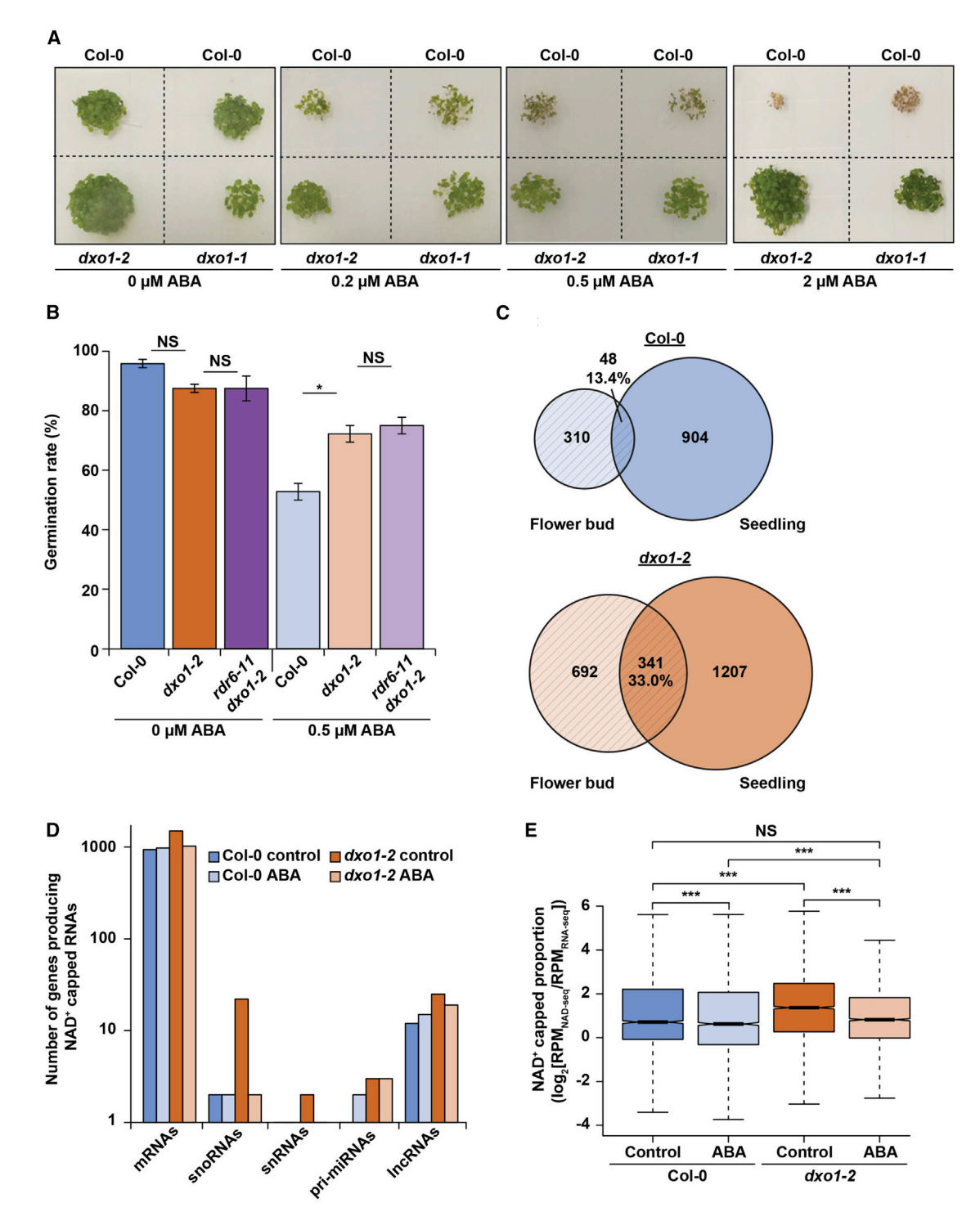


Figure 4. DXO1 Is Required for Proper ABA Response, and This Plant Hormone Remodels the NAD+ Capped Transcriptome

(A) Representative images of seed germination of Col-0, dxo1-1, and dxo1-2 7-day-old seedlings with 0, 0.2, 0.5, and 2 μM ABA.

(B) Seed germination rate of Col-0 (blue bars), dxo1-2 single (orange bars), and rdr6-11 dxo1-2 double (purple bars) mutant 4-day-old seedlings with 0 μM (dark colors) and 0.5 µM ABA (shaded colors). Error bars indicate ± standard error of the mean. NS denotes no significance, and * denotes p value < 0.05, respectively, Student's t test.

(C) The overlap of NAD*-capped RNAs identified in unopened flower buds (light striped colors) or 12-day-old seedlings (dark colors) of Col-0 (blue circles) and dxo1-2 (orange circles), respectively.

(legend continued on next page)





NAD+ is a ubiquitous coenzyme in eukaryotic cell redox reactions. Thus, the NAD+ cap modification on mRNA transcripts provides a potential link between NAD+ metabolism and posttranscriptional regulation (Figures 1D and S2F; Kiledjian, 2018). We hypothesized that loss of DXO1 decapping function would result in NAD+ being trapped on mRNAs, and thus, lead to increased NAD+ biogenesis to restore free NAD+ levels. To test this, we performed quantitative liquid chromatography-high resolution mass spectrometry (LC-HRMS) (Frederick et al., 2017) to measure global levels of free NAD+ in Col-0 and dxo1-2 single mutant seedlings. We found that there was no significant difference in the total NAD+ levels between Col-0 and dxo1 single mutant plants, indicating that loss of DXO1 does not increase total NAD+ levels (Figure 3D). Given that RDR6-dependent PTGS targets NAD+-capped RNAs in the absence of DXO1, we measured NAD+ levels in rdr6-11 dxo1-2 plants. We found that total NAD+ levels were significantly (p values < 0.05, Student's t test) increased in rdr6-11 dxo1-2 double mutant plants as compared with both Col-0 and dxo1-2 single mutant plants (Figure 3D). This increase suggests that when NAD+ cannot be removed from mRNAs in the absence of both DXO1-mediated decapping and RDR6-directed smRNA processing of NAD+capped transcripts, plants increase total NAD+ levels.

In plants, the NAD+ biosynthesis pathways include de novo and salvage pathways (Hashida et al., 2009). The de novo pathway requires several enzymes, including quinolinate phosphoribosyltransferase (QPRT), nicotinate/nicotinamide mononucleotide adenylyltransferase (NMNAT), and NAD+ synthetase (NADS) to convert aspartate to NAD+, while NMNAT is common to both pathways (Hashida et al., 2009) (Figure 3E). To test if the levels of mRNAs encoding these enzymes increase in response to a lack of NAD+ cap removal, we examined the abundance of the transcripts encoding these three enzymes using RT-qPCR and found that transcripts encoding the first two proteins required for NAD+ biosynthesis (QPRT and NMNAT) were both significantly (p values < 0.01. Student's t test) more abundant in dxo1-2 single and rdr6-11 dxo1-2 double mutant plants as compared with Col-0 (Figure 3F). Notably, the double mutant had significantly (p values < 0.05, Student's t test) higher levels of both mRNAs compared with dxo1-2 single mutants (Figure 3F). The transcript encoding the final enzyme required for NAD+ biosynthesis (NADS) was significantly (p value < 0.05, Student's t test) more abundant only in rdr6-11 dxo1-2 double mutant plants as compared with both Col-0 and dxo1-2 single mutants (Figure 3F). These results indicate that when NAD+-capped RNAs are not decapped by DXO1 or processed into RDR6-dependent smRNAs, transcripts encoding the proteins required for the final stage of the salvage and the last three steps of de novo NAD⁺ biosynthesis are specifically increased.

DXO1 Is Required for Proper Plant Response to ABA during Seed Germination

We found that a collection of DXO1-dependent NAD+-capped mRNAs were enriched in those encoding proteins involved in the plant response to ABA (Figure 1E), so we hypothesized

that DXO1 function may be required for proper plant response to ABA during seed germination. We measured the germination efficiency of Col-0 and both mutant alleles of dxo1 with increasing concentrations of ABA (0, 0.2, 0.5, and 2 μM). As expected, Col-0 seed germination was sensitive to increasing ABA levels, as fewer seeds germinated in a concentration-dependent manner (Figure 4A). Conversely, dxo1 mutant seeds were insensitive to the varying ABA concentrations, as they continued germinating in the presence of increasing ABA levels compared with Col-0 (Figure 4A). In fact, dxo1 mutant seeds were able to germinate when the ABA concentration was as high as 10 μM (Figure S5A), indicating the importance of DXO1 for proper ABA response during plant seed germination.

Given the role of RDR6-dependent smRNA processing in NAD+-capped transcript destabilization, we measured seed gemination for Col-0, dxo1-2 single, and rdr6-11 dxo1-2 double mutant plants without and with 0.5 μM ABA. We found that dxo1-2 single and rdr6-11 dxo1-2 double mutant seeds both displayed similar ABA insensitivity as compared with Col-0 upon exposure to increased ABA levels (Figure 4B). These results indicate that both the developmental defects and insensitivity to ABA seed germination inhibition of dxo1-2 plants is not a result of the PTGS-mediated smRNA processing of NAD+-capped mRNAs.

Exposure to ABA Leads to Global Remodeling of the NAD*-Capped Transcriptome

We next set out to determine the effect of this hormone on the NAD+-capped transcriptome. To examine this, we performed NAD-seq and total RNA-seq on 12-day-old Col-0 and dxo1 seedlings treated without and with 0.5 μ M ABA, producing \sim 14-22 million total reads per library. The biological replicates of each library type from the distinct genotypes and treatments clustered together (Figures S5B and S5C), indicating the high quality and reproducibility of our libraries. In Col-0 seedlings, we detected 952 and 995 genes producing NAD+-capped transcripts under control and 0.5 µM ABA conditions, respectively. In dxo1 mutant seedlings, we identified 1,548 and 1,048 genes producing NAD+-capped transcripts under control and 0.5 μM ABA conditions, respectively (Tables S4, S5, S6, and S7). To interrogate the developmental specificity of NAD+ capping in the Arabidopsis transcriptome, we compared NAD+-capped transcripts between unopened flower buds and 12-day-old seedlings in both Col-0 and dxo1 mutants. We found that only 13.4% and 33% of NAD⁺-capped transcripts in flower buds from Col-0 and dxo1 single mutants, respectively, were also detected in seedlings of these same genotypes (Figure 4C), indicating NAD+ capping is indeed regulated in a developmental-specific manner.

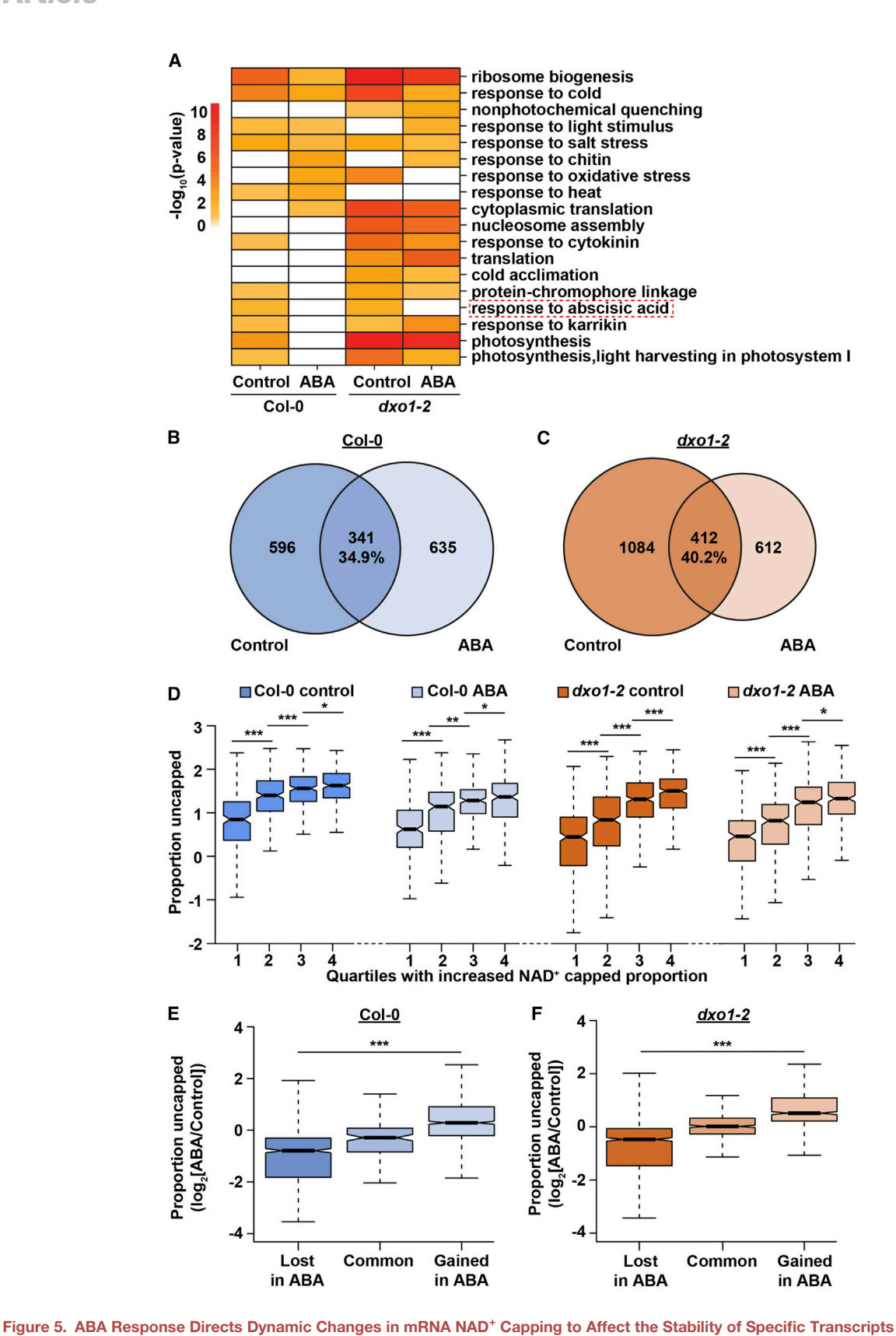
As for unopened flower buds, the majority of NAD+-capped transcripts detected in 12-day-old seedlings were protein-coding mRNAs in both conditions (± ABA). Additionally, we also detected some NAD+-capped pri-miRNAs, snoRNAs, and other IncRNAs in these younger plant tissues (Figure 4D; Tables S4, S5, S6, and S7). Notably, there were more snoRNAs with a significant NAD+-capped proportion value present in 12-day-old

⁽D) The number of genes producing NAD*-capped transcripts identified in Col-0 and dxo1-2 mutant 12-day-old seedlings both without and with 0.5 μM ABA treatment for the different specified categories.

⁽E) NAD+-capped proportion for Col-0 and dxo1-2 mutant 12-day-old seedlings without and with 0.5 μM ABA treatment. *** denotes p value < 0.001 and NS denotes no significance, Mann-Whitney U test.

Article





(A) The list of biological process GO terms that are enriched (p value < 0.01) in at least two of the four indicated conditions. The color bar indicates the $-\log_{10}(p)$ value) of the enrichment for that condition. White boxes indicate no enrichment.





dxo1 seedlings compared with Col-0 under control conditions (Figure 4C), which was different than in the unopened flower buds, where snoRNAs were also present in Col-0 (Figure 1D). In fact, this class of NAD+-capped transcripts were reduced to Col-0 levels (mostly disappeared) in dxo1 mutant seedlings upon 0.5 μM ABA treatment. Additionally, some pri-miRNA transcripts were also modified with a NAD+ cap. In both Col-0 and dxo1 seedlings, we identified NAD+-capped primary MIR167D, MIR167A, MIR158A, and MIR398C, but their levels of NAD+ capping and treatment under which this modification occurred varied for these RNAs (Figure S5D; Tables S4, S5, S6, and S7). For instance, primary MIR158A was only found in a NAD+-capped form in Col-0 seedlings when they were treated with 0.5 μM ABA, while this RNA was significantly (adjusted p value < 0.01) more NAD+-capped in dxo1 seedlings with and without ABA treatment as compared with Col-0 (Figure S5D; Tables S4, S5, S6, and S7). A similar pattern was noted for primary MIR398C, with the only difference being that this MIRNA was only NAD+-capped in Col-0 seedlings when they were not treated with ABA (Figure S5D; Tables S4, S5, S6, and S7). These findings suggest a potential link between this non-canonical cap modification and miRNA processing.

To investigate the magnitude by which ABA response remodels the landscape of plant transcriptome NAD+ capping, we directly compared the NAD+-capped proportion (log₂[RPM_{NAD-seq}/ RPM_{RNA-sed}]) values for the entire Col-0 and dxo1 transcriptomes before and during ABA treatment. Using this metric, we found that transcripts with NAD+ caps were significantly (p value < 0.001, Mann-Whitney U test) more abundant in dxo1 mutant seedlings relative to Col-0 both with and without ABA treatment (Figure 4E), consistent with our original results in unopened flower buds (Figure S2F). These results also revealed that DXO1 regulates numerous NAD+-capped transcripts in the Arabidopsis seedling transcriptome with and without ABA treatment (Figures 4D and 4E). Specifically, we found that the overall levels of NAD+-capped transcripts were significantly (p value < 0.001, Mann-Whitney U test) decreased in both genotypes when they were treated with ABA compared with not treated (Figure 4E), indicating a global loss in NAD+ capping during ABA treatment. In fact, this analysis revealed that the levels of overall NAD+ capping in dxo1 mutant seedlings during ABA response were reduced to levels similar to those identified in Col-0 prior to ABA treatment (Figure 4E; compare the dark blue box to the light orange box). These results indicate that the plant ABA response directs a global decrease of NAD+ capping in the plant transcriptome that is mostly DXO1-independent.

The Stability of Transcripts Encoding Master Regulators of ABA Response Is Dynamically Regulated by NAD⁺ **Capping upon ABA Treatment**

To determine the biological functionality of proteins encoded by the NAD+-capped mRNAs that dynamically respond to ABA, we

performed GO term analysis. We found that NAD+-capped transcripts in both conditions and genotypes were enriched for those encoding proteins involved in ribosome biogenesis, response to cold, and response to salt (Figure 5A), revealing that these classes of transcripts are consistently NAD+ capped in 12-day-old seedlings. Our results also showed that mRNAs encoding proteins involved in plant response to ABA were modified with a 5' NAD+ cap in both Col-0 and dxo1 mutant seedlings in the absence of ABA treatment (Figure 5A), possibly to destabilize these transcripts in the absence of this hormone. Conversely, when seedlings of these same genotypes were treated with ABA, the majority of the population of ABA response protein encoding transcripts lost their 5' NAD+ caps (Figure 5A), demonstrating that this modification can be potentially used as a dynamic transcriptome addition to regulate specific transcript sets to affect eukaryotic physiological responses.

To test the idea that NAD+ caps can act as dynamic regulators of mRNA stability, we performed GMUCT in both Col-0 and dxo1 mutant 12-day-old seedlings under control and ABA conditions. The GMUCT libraries were sequenced and provided ~7-18 million mapped reads, and the biological replicates from the distinct genotypes and treatments clustered together (Figure S5E), indicating the high quality and reproducibility of these libraries. Using the proportion uncapped metric, we found that overall the RNAs with high NAD+-capped proportion values tended to be significantly (p values < 0.001, Mann-Whitney U test) more unstable in all these samples (Figure 5D). In fact, when these collections of NAD+-capped transcripts were separated into quartiles based on their increasing NAD+-capped proportion (log₂[RPM_{NAD-seq}/RPM_{RNA-seq}]) values (quartile 1 lowest and 4 highest), we observed significant (all p values < 0.05, Mann-Whitney *U* test) monotonic increases in their proportion uncapped values in both Col-0 and dxo1-2 mutant seedlings (Figure 5D). Thus, the levels of transcript stability from the identified NAD+-capped transcripts decreased as a function of the levels of the total transcript pool identified with a NAD+ cap for each given mRNA.

We then calculated proportion uncapped fold change (log₂[ABA/control]) for each genotype and examined this metric for transcripts that gain, lose, or maintain (common) their NAD+ capping status in these two genotypes in the context of ABA response (Figures 5E and 5F). We found that 802 and 1,084 mRNAs significantly decreased (lost) and 841 and 612 mRNAs that significantly increased (gained) proportion NAD+ capping during ABA response in Col-0 and dxo1 plants, respectively (Figures 5B and 5C). We compared these collections of transcripts to those transcripts that maintained NAD+ capping in both conditions (341 in Col-0 and 412 in dxo1 (common)). From this analysis, we found that in both Col-0 and dxo1 mutant seedlings, transcripts that lost NAD+ caps during ABA treatment had significantly (p value < 0.001, Mann-Whitney U

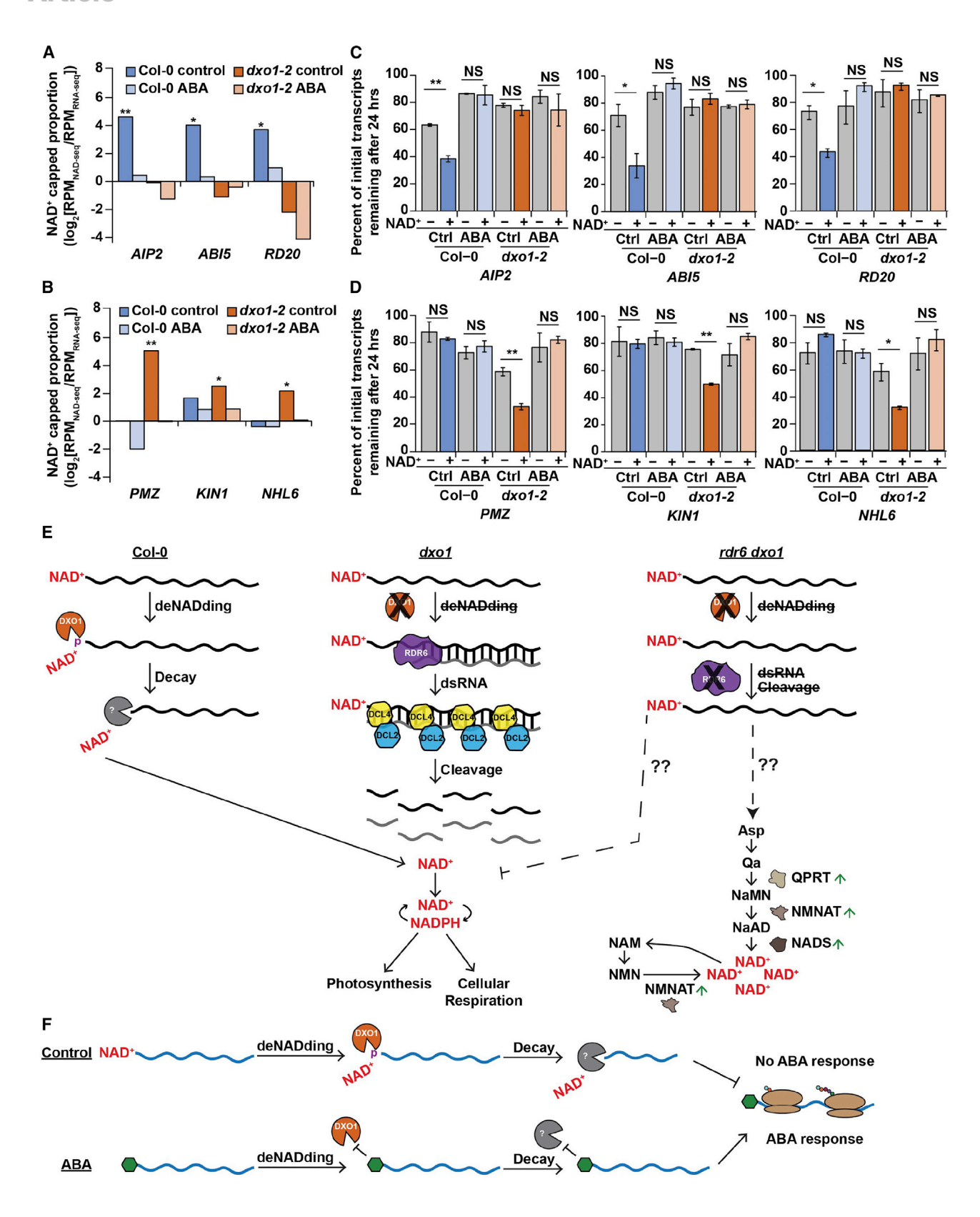
⁽B and C) The overlap of NAD*-capped RNAs identified in 12-day-old Col-0 seedlings (B) and dxo1-2 seedlings (C) without (dark circle) and with 0.5 µM ABA (light circle) treatment.

⁽D) The proportion uncapped values for four quartiles of NAD*-capped transcripts based on increasing levels of NAD*-capped proportion values, with quartile 1 having the lowest values and 4 having the highest in Col-0 and dxo1-2 mutant seedlings without and with ABA treatment. *, **, and *** denote p value < 0.05, 0.01, and 0.001, respectively, Mann-Whitney U test.

⁽E and F) The proportion uncapped fold change (log₂[ABA/control]) values for transcripts that lose NAD+ capping (Left), maintain their NAD+ capping (Middle), or gain NAD+ capping (Right) in Col-0 (E) and dxo1-2 (F) seedlings during ABA treatment as compared with before. *** denotes p value < 0.001, Mann-Whitney U test.

Article





(legend on next page)





test) lower proportion uncapped (more stable) than those transcripts that maintained this moiety in both conditions (Figures 5D and 5E), revealing that transcripts that no longer had a NAD+ cap during ABA response were stabilized in this process in Col-0 and *dxo1-2* plants. Conversely, transcripts that gained a NAD+ cap during ABA response demonstrated the exact opposite pattern and were destabilized during ABA treatment in both Col-0 *and dxo1-2* plants (Figures 5D and 5E). These results reveal that the NAD+ cap modification can be used as a dynamic transcriptome addition to decrease the stability of specific sets of transcripts during eukaryotic physiological responses.

Finally, we looked specifically at the subset of NAD+-capped transcripts that are known to be required for plant ABA response (response to ABA GO term) (Figure 5A). We found that 13 of these mRNAs were significantly (p value < 0.05, edgeR) NAD+ capped in Col-0 without ABA treatment (Figures 6A and S6A), and this modification was reduced or lost when these plants were treated with ABA. These 13 mRNAs displayed a reduced level or completely lost NAD+ capping in dxo1 mutant seedlings during both conditions (Figures 6A and S6A), thus in the absence of DXO1 function these mRNAs did not demonstrate dynamic NAD+ capping as occurred in Col-0 plants during ABA response. We also identified 15 other mRNAs encoding ABA response proteins that displayed this dynamic pattern of NAD+ capping in dxo1 mutant seedlings, which was mostly absent in Col-0 seedlings (Figures 6B and S6B). In fact, all 28 of these mRNAs encoding ABA response proteins displayed reduced or absent NAD+ capping during ABA treatment in both genotypes (Figures 6A, 6B, S6A, and S6B).

Our proportion uncapped analyses suggest that ABA-directed NAD⁺ capping can dynamically regulate mRNA stability (Figures 5D and 5E). Thus, the mRNAs encoding ABA response proteins that showed a loss of NAD⁺ capping in response to ABA treatment in Col-0 and *dxo1* mutant seedlings should display decreased stability when the NAD⁺ cap was present and vice versa. To further test this, we treated Col-0 and *dxo1* seedlings with the transcription inhibitors cordycepin and actinomycin D for 0 and 24 h before and during ABA response. We then tested the stability of three transcripts that demonstrate a dynamic decrease in NAD⁺ capping in response to ABA in Col-0 (*ABI5* (*AT2G36270*), *AIP2* (*AT5G20910*), and *RD20* (*AT2G33380*)) (Figures 6A and 6C) or in *dxo1* (*PMZ* (*AT3G28210*), *KIN1*

(AT5G15960), and NHL6 (AT1G65690)) (Figures 6B and 6D) seedlings by calculating the percentage of initial transcripts remaining 24 h after treatment using RT-qPCR. As expected, we found that significantly (p value < 0.05, Student's t test) less transcript remained 24 h after transcription inhibition before as compared with after ABA treatment in Col-0 for ABI5, AIP2, and RD20 (Figure S6C), as well as in dxo1 mutant seedlings for PMZ, KIN1, and NHL6 (Figure S6D). These findings revealed that the stability of these total transcript pools was significantly lower in the absence of treatment with this phytohormone when their NAD+ capping levels were significantly higher (Figures 6A and 6B). We also wanted to validate specifically that it was the NAD+-capped portion of the transcript population that was destabilized for these specific transcripts (Figure 5D). To do this, we performed NAD+ capture to distinguish NAD+-capped transcripts from the other portion of transcripts for these same six mRNAs following the same treatments with the transcription inhibitors for 0 and 24 h in samples without and with ABA treatment. We found that the levels of NAD+-capped transcripts were significantly (p value < 0.05, Student's t test) lower 24 h after transcription inhibitor treatment as compared with the other portions of these mRNAs in Col-0 without ABA treatment for ABI5, AIP2, and RD20 (Figure 6C), as well as in dxo1 mutant seedlings without ABA treatment for PMZ, KIN1, and NHL6 (Figure 6D). Thus, the NAD+-capped portion of these transcripts specifically displayed significantly decreased stability in the absence of ABA treatment when their overall levels are lower (Figures 6A and 6B). Ultimately, these findings reveal a previously uncharacterized and essential role of mRNA NAD+ capping in dynamically regulating the stability of transcripts encoding specific regulators to allow proper ABA response.

DISCUSSION

The NAD*-Capped Transcriptome Is Controlled in a Developmental-Dependent Manner

We used NAD-seq to study the NAD⁺-capped portion of the Arabidopsis unopened flower bud and 12-day-old seedling with and without ABA treatment transcriptomes for both Col-0 and *dxo1* mutant plants. This analysis revealed that NAD⁺-capped RNAs accumulated in the absence (*dxo1* mutant) as compared with the presence (Col-0) of DXO1 function (Figures 1A, 1B, 4B, and

Figure 6. Transcripts Encoding Master Regulators of ABA Response Have Their Stability Dynamically Regulated by NAD* Capping upon ABA Treatment

(A and B) NAD*-capped proportion in Col-0 (blue bars) and dxo1-2 (orange bars) in the absence (darker colors) or presence (lighter colors) of ABA for ABA-responsive mRNAs that specifically contain a NAD* cap in Col-0 (A) or dxo1-2 (B). * and ** denote p value < 0.05 and 0.01, respectively, negative binomial generalized linear model.

(C and D) Percent of total ABI5, AIP2, and RD20 (C) and PMZ, KIN1, and NHL6 (D) without (–) and with (+) NAD⁺ caps remaining 24 h post treatment with transcription inhibitors in Col-0 and dxo1-2 mutant seedlings without and with ABA treatment. NS denotes no significance. * and ** denote p value < 0.05 and 0.01, respectively, Student's t test. Error bars indicate ± standard error of the mean.

(E) A model illustrating the link among DXO1-mediated deNADding, small RNA biosynthesis, and NAD+ biosynthesis. (Left) In Col-0 plants, the NAD+-capped transcripts are deNADed by DXO1, releasing the NAD+ into the free NAD+ pool. (Middle) In dxo1 mutant plants, NAD+-capped transcripts cannot be deNADed by DXO1, and thus, are subject to RDR6-dependent PTGS, which releases the NAD+ cap into the free NAD+ pool. (Right) In rdr6 dxo1 double mutant plants, the NAD+ transcripts cannot be deNADed by DXO1 or turned into smRNAs by RDR6-mediated PTGS. Thus, the NAD+ cap is likely not permitted re-entry to the NAD+ pool, which may trigger an unknown feedback regulatory mechanism to increase abundance of the mRNAs encoding the NAD+ biosynthetic enzymes, including QPRT, NMNAT, and NADS, ultimately resulting in the increase of total free NAD+.

(F) A model illustrating the dynamic NAD⁺ capping changes in the transcriptome before and during ABA response. During normal conditions, the ABA-responsive transcripts (blue) are marked by NAD⁺ caps, which are deNADed by DXO1 and are subsequently degraded, resulting in no ABA response. During ABA treatment, ABA-responsive transcripts lack the NAD⁺ cap (likely resulting in inclusion of the canonical m⁷G cap instead), which increases their stability and permits proper plant response to ABA

Article



4D), indicating that DXO1 acts *in vivo* as a deNADding enzyme for the plant transcriptome. Among the DXO1 deNADding substrates identified in Arabidopsis were snoRNAs (Figures 1D and 4D), which is consistent with the findings in human cells (Jiao et al., 2017). In fact, we found that DXO1 deNADed a number of snoRNAs in a tissue-specific manner (Figures 1D and 4D), suggesting this 5' end modification may play a developmental or tissue-specific regulatory function on this class of non-coding RNAs in plant. This idea was also supported by the minimal overlap in the NAD+capped mRNAs identified in Arabidopsis unopened flower buds as compared with 12-day-old seedlings (Figure 4C).

One of the DXO1 deNADding substrates that had not been previously observed in other systems, were several primary MIRNA transcripts, including MIR158A, MIR167A, MIR167D, and MIR169J, which were not identified in unopened flower buds but specifically in 12-day-old seedlings that had or had not been treated with 0.5 μM ABA (Figures 4D and S5D; Tables S4, S5, S6, and S7), while MIR398C was the only one detected in both tissues (Figure 1D; Tables S4, S5, S6, and S7). Recent studies have linked a different reversible covalent RNA modification (N⁶-methyladenosine (m⁶A)) to primary miRNA processing (Alarcón et al., 2015; Bhat et al., 2020), suggesting that future experiments should explore a role for 5' end NAD+ capping in miRNA processing. In total, our findings revealed that 5' end NAD+ capping regulates specific subsets of the transcriptome in a tissue-specific manner and may be an important regulatory mechanism throughout development.

RDR6-Dependent PTGS Processes NAD*-Capped Transcripts into smRNAs in the Absence of DXO1

In human cells, NAD+-capped mRNAs tend to be more abundant when the function of DXO1 is absent (Jiao et al., 2017). However, our RNA-seq analyses in both plant tissues found that NAD+-capped mRNAs were not present at significantly different levels in the absence (dxo1 mutant) as compared with the presence (Col-0) of DXO1 function (Figures 2A and 2B). Relatedly, we found that NAD+-capped RNAs were less stable in Arabidopsis both with and without functionally active DXO1 (both Col-0 and dxo1 mutant plants, respectively) (Figures 2C, 5D, and 5E). Thus, it is clear that 5' end NAD+ capping is also a destabilizing mark in plant transcriptomes, but it was unclear what pathway was driving the instability of these transcripts in the absence of DXO1 (dxo1 mutants). Two recent studies had found that in dxo1 mutant plants a large collection of mRNAs (> 1,000) were processed into RDR6dependent smRNAs (Kwasnik et al., 2019; Pan et al., 2020), and we observed the same phenomenon (Figures 3A-3C and S4B-S4D). In fact, we found that this pathway for smRNA processing was producing smRNAs from NAD+-capped mRNAs, likely acting as an alternative degradation pathway (Figure 6E). These findings have revealed the intriguing observation that RDR-mediated smRNA processing can be utilized as a bona fide mechanism for breaking down mRNAs containing non-canonical 5' caps and opened up an area of future research inquiry.

The existence of a potential backup mechanism for breaking down 5' NAD⁺-capped mRNAs through smRNA processing, suggested that reacquiring the 5' end NAD⁺ from these modified mRNAs is an important physiological process. It also led to the question of how plants respond if both of these degradation mechanisms are missing. Therefore, we determined the overall

NAD⁺ levels in Col-0, *dxo1* single, and *rdr6 dxo1* double mutants, and found that overall NAD⁺ levels were increased only when both pathways for NAD⁺-capped RNA destabilization were lost (Figure 3D). These results suggested the existence of a feedback pathway for sensing available NAD⁺ molecules, and our observation that the transcripts encoding three proteins required for downstream steps of NAD⁺ biosynthesis are significantly more abundant in plants that lack both RDR6 and DXO1 (*rdr6 dxo1* double mutants) compared with when one or both are functional (Figures 3E and 3F) also provides initial support for this hypothesis. Future research efforts will be required to identify and characterize the components and mechanisms involved in such a NAD⁺ cap sensing and feedback pathway (Figure 6E).

NAD* Capping Is a Dynamic Epitranscriptome Mark Tagging Specific Transcripts for Degradation during Plant ABA Response

The NAD-seq analysis in unopened flower buds showed that a subset of DXO1 deNADding targets encoded proteins required for proper ABA response (Figure 1E), suggesting that this de-NADding enzyme functions in ABA regulation of seed germination. We tested this hypothesis and found that indeed DXO1 is required for proper ABA response (Figures 4A and S5A). This phenotype was not a byproduct of the RDR6-dependent smRNAs produced from NAD+-capped mRNAs in the absence of DXO1 function (Figure 4B), suggesting that 5' end NAD+ capping was required for proper ABA response in plants. Our NAD-seq in Col-0 and dxo1 mutant seedlings with and without ABA treatment revealed that the overall levels of NAD+ capping decreased in both genotypes (Figure 4E), but especially in dxo1 mutant seedlings where the number of total genes producing NAD+-capped RNAs decreased (Figure 4D). Thus, ABA treatment results in significant and dynamic changes to the NAD+capped transcriptome in plants, revealing that this, like other RNA modifications (e.g., m⁶A) (Anderson et al, 2018; Nachtergaele and He, 2017), can be added and removed from specific RNAs in response to specific physiological conditions.

A major collection of mRNAs that displayed a significant decrease in NAD+ capping levels in both Col-0 and dxo1 mutant seedlings were those encoding regulators of ABA response (Figures 5A, 6A, 6B, S6A, and S6B). Given that NAD+ capping is a destabilizing mark when present on Arabidopsis mRNAs (Figures 2C, 5D, 5E, 6C, 6D, S6C, and S6D), we reasoned that the dynamic loss of NAD+ caps would result in the stabilization of these transcripts in response ABA treatment. As expected, we found that the dynamic loss of NAD+ caps during ABA response significantly increased stability of the corresponding transcripts and vice versa (Figures 5D, 5E, 6C, 6D, S6C, and S6D). Relatedly, a collection of 28 transcripts encoding ABA response proteins displayed interesting patterns of NAD+ capping dynamics in response to ABA treatment in the absence of DXO1 function (in dxo1 mutant seedlings) (Figures 6A, 6B, S6A, and S6B). This overall improper regulation of such a large collection of mRNAs encoding ABA response proteins provides a compelling explanation for the ABA hyposensitivity of dxo1 mutant plants (Figures 4A, 4B, and S5A). Furthermore, the decrease in 5' NAD+ capping of these 28 mRNAs in dxo1 mutant plants (Figures 6A, 6B, S6A, and S6B) reveals that this dynamic response does not require the functionality of DXO1. Thus, the dynamic regulation of 5' end





Developmental CellArticle

NAD⁺ capping during ABA response could be directed by another enzyme(s) with deNADding activity, which are prevalent in the Arabidopsis genome (Yoshimura and Shigeoka, 2015), or by the machinery responsible for adding this epitranscriptome mark in eukaryotic transcriptomes, with neither of these models being mutually exclusive. In conclusion, our study reveals that plant ABA response remodels the NAD⁺-capped transcriptome even in the absence of DXO1 function (Figure 6F), thus providing evidence that mRNA NAD⁺ caps can be dynamically regulated to affect a eukaryotic physiological response.

STAR*METHODS

Detailed methods are provided in the online version of this paper and include the following:

- KEY RESOURCES TABLE
- RESOURCE AVAILABILITY
 - Lead Contact
 - Materials Availability
 - Data and Code Availability
- EXPERIMENTAL MODEL AND SUBJECT DETAILS
 - Plant Materials
 - Generation of pDXO1::DXO1-GUS::DXO1-3'UTR dxo1-2 Plants
 - Generation of pUBQ10::DXO1-eGFP dxo1-2 Plants
- METHOD DETAILS
 - Histochemical Analysis of pDXO1::DXO1-GUS dxo1-2
 Plants
 - DXO1 Subcellular Localization Analysis Using pUBQ10::DXO1-eGFP/dxo1-2 Plants
 - Validation of NAD⁺ Capture Approach Using *In Vitro* Luciferase Transcription
 - RNA Extraction
 - O In Vivo NAD-seg Library Construction
 - Validation of NAD-seq by NAD-qPCR
 - polyA-selected and Total RNA-seq (mRNA- and RNAseq) Library Construction
 - smRNA-seq Library Construction
 - Genome-wide Mapping of Uncapped and Cleaved Transcripts (GMUCT)
 - Germination Test during ABA Treatment
 - Liquid Chromatography-High Resolution Mass Spectrometry (LC-HRMS) to Detect Total NAD⁺
 - gRT-PCR to Detect NAD+ Biosynthesis Genes
 - Transcript Stability Time Course
- QUANTIFICATION AND STATISTICAL ANALYSIS
 - Identification of NAD⁺ Capped RNAs
 - Measurement of mRNA Stability Using the Proportion Uncapped Metric
 - O Differential Abundance Analysis
 - Small RNA Profiling
 - Determination of Library Reproducibility
 - O Construction of a DXO1 Phylogenetic Tree

SUPPLEMENTAL INFORMATION

Supplemental Information can be found online at https://doi.org/10.1016/j.devcel.2020.11.009.

ACKNOWLEDGMENTS

The authors would like to thank members of the B.D.G. lab, both past and present for helpful discussions. This work was funded by NSF, United States grants IOS-2023310 and IOS-1849708 to B.D.G. and R01GM132261 to N.W.S.; S.T. is supported by the American Diabetes Association, United States through post-doctoral fellowship 1-19-PDF-144. The funders had no role in study design, data collection and analysis, decision to publish, or preparation of the manuscript.

AUTHOR CONTRIBUTIONS

B.D.G. conceived the study. X.Y., M.R.W., S.T., N.W.S., and B.D.G. designed the experiments. X.Y., M.R.W., L.E.V., S.T., J.S., R.G., N.W.S., and B.D.G. performed experiments. X.Y., S.T., M.C.K., N.W.S., E.L., and B.D.G. analyzed the data. X.Y., M.C.K., and B.D.G. wrote the paper with assistance from all authors. The authors have read and approved the manuscript for publication.

DECLARATION OF INTERESTS

The authors declare no competing interests.

Received: May 20, 2020 Revised: September 2, 2020 Accepted: November 6, 2020 Published: December 7, 2020

REFERENCES

Alarcón, C.R., Lee, H., Goodarzi, H., Halberg, N., and Tavazoie, S.F. (2015). N6-methyladenosine marks primary microRNAs for processing. Nature *519*, 482–485.

Anders, S., Pyl, P.T., and Huber, W. (2015). HTSeq–a Python framework to work with high-throughput sequencing data. Bioinformatics *31*, 166–169.

Anderson, S.J., Kramer, M.C., Gosai, S.J., Yu, X., Vandivier, L.E., Nelson, A.D.L., Anderson, Z.D., Beilstein, M.A., Fray, R.G., Lyons, E., and Gregory, B.D. (2018). N6-methyladenosine inhibits local ribonucleolytic cleavage to stabilize mRNAs in Arabidopsis. Cell Rep. 25, 1146–1157.e3.

Baulcombe, D.C. (1996). Mechanisms of pathogen-derived resistance to viruses in transgenic plants. Plant Cell 8, 1833–1844.

Bhat, S.S., Bielewicz, D., Gulanicz, T., Bodi, Z., Yu, X., Anderson, S.J., Szewc, L., Bajczyk, M., Dolata, J., Grzelak, N., et al. (2020). mRNA adenosine methylase (MTA) deposits m ⁶ A on pri-miRNAs to modulate miRNA biogenesis in *Arabidopsis thaliana*. Proc. Natl. Acad. Sci. USA *117*, 21785–21795.

Bird, J.G., Basu, U., Kuster, D., Ramachandran, A., Grudzien-Nogalska, E., Towheed, A., Wallace, D.C., Kiledjian, M., Temiakov, D., Patel, S.S., et al. (2018). Highly efficient 5' capping of mitochondrial RNA with NAD⁺ and NADH by yeast and human mitochondrial RNA polymerase. eLife 7, e42179.

Bird, J.G., Zhang, Y., Tian, Y., Panova, N., Barvík, I., Greene, L., Liu, M., Buckley, B., Krásný, L., Lee, J.K., et al. (2016). The mechanism of RNA 5' capping with NAD+, NADH and desphospho-CoA. Nature 535, 444–447.

Cahová, H., Winz, M.L., Höfer, K., Nübel, G., and Jäschke, A. (2015). NAD captureSeq indicates NAD as a bacterial cap for a subset of regulatory RNAs. Nature *519*, 374–377.

Chang, J.H., Jiao, X., Chiba, K., Oh, C., Martin, C.E., Kiledjian, M., and Tong, L. (2012). Dxo1 is a new type of eukaryotic enzyme with both decapping and 5'-3' exoribonuclease activity. Nat. Struct. Mol. Biol. 19, 1011–1017.

Chen, Y.G., Kowtoniuk, W.E., Agarwal, I., Shen, Y., and Liu, D.R. (2009). LC/MS analysis of cellular RNA reveals NAD-linked RNA. Nat. Chem. Biol. 5, 879–881.

Chiu, W., Niwa, Y., Zeng, W., Hirano, T., Kobayashi, H., and Sheen, J. (1996). Engineered GFP as a vital reporter in plants. Curr. Biol. 6, 325–330.

Dobin, A., Davis, C.A., Schlesinger, F., Drenkow, J., Zaleski, C., Jha, S., Batut, P., Chaisson, M., and Gingeras, T.R. (2013). STAR: ultrafast universal RNA-seq aligner. Bioinformatics 29, 15–21.

Article



Donnelly, P.M., Bonetta, D., Tsukaya, H., Dengler, R.E., and Dengler, N.G. (1999). Cell cycling and cell enlargement in developing leaves of Arabidopsis. Dev. Biol. 215, 407-419.

Finkelstein, R. (2013). Abscisic acid synthesis and response. Arabidopsis Book

Frederick, D.W., Trefely, S., Buas, A., Goodspeed, J., Singh, J., Mesaros, C., Baur, J.A., and Snyder, N.W. (2017). Stable isotope labeling by essential nutrients in cell culture (SILEC) for accurate measurement of nicotinamide adenine dinucleotide metabolism. Analyst 142, 4431-4437.

Frindert, J., Zhang, Y., Nübel, G., Kahloon, M., Kolmar, L., Hotz-Wagenblatt, A., Burhenne, J., Haefeli, W.E., and Jäschke, A. (2018). Identification, biosynthesis, and decapping of NAD-capped RNAs in B. subtilis. Cell Rep. 24, 1890-

Gonatopoulos-Pournatzis, T., and Cowling, V.H. (2014). Cap-binding complex (CBC). Biochem. J. 457, 231-242.

Gosai, S.J., Foley, S.W., Wang, D., Silverman, I.M., Selamoglu, N., Nelson, A.D.L., Beilstein, M.A., Daldal, F., Deal, R.B., and Gregory, B.D. (2015). Global analysis of the RNA-protein interaction and RNA secondary structure landscapes of the Arabidopsis nucleus. Mol. Cell 57, 376-388.

Gregory, B.D., O'Malley, R.C., Lister, R., Urich, M.A., Tonti-Filippini, J., Chen, H., Millar, A.H., and Ecker, J.R. (2008). A link between RNA metabolism and silencing affecting Arabidopsis development. Dev. Cell 14, 854-866.

Hashida, S.N., Takahashi, H., and Uchimiya, H. (2009). The role of NAD biosynthesis in plant development and stress responses. Ann. Bot. 103, 819-824.

Herr, A.J., Molnàr, A., Jones, A., and Baulcombe, D.C. (2006). Defective RNA processing enhances RNA silencing and influences flowering of Arabidopsis. Proc. Natl. Acad. Sci. USA 103, 14994-15001.

Huang, da W., Sherman, B.T., and Lempicki, R.A. (2009). Systematic and integrative analysis of large gene lists using DAVID bioinformatics resources. Nat. Protoc. 4, 44-57.

Hugouvieux, V., Kwak, J.M., and Schroeder, J.I. (2001). An mRNA cap binding protein, ABH1, modulates early abscisic acid signal transduction in Arabidopsis. Cell 106, 477-487.

Jiao, X., Doamekpor, S.K., Bird, J.G., Nickels, B.E., Tong, L., Hart, R.P., and Kiledjian, M. (2017). 5' End nicotinamide adenine dinucleotide Cap in human cells promotes RNA decay through DXO-Mediated deNADding. Cell 168, 1015-1027.e10.

Kiledjian, M. (2018). Eukaryotic RNA 5'-end NAD + capping and DeNADding. Trends Cell Biol. 28, 454-464.

Klepikova, A.V., Kasianov, A.S., Gerasimov, E.S., Logacheva, M.D., and Penin, A.A. (2016). A high resolution map of the Arabidopsis thaliana developmental transcriptome based on RNA-seq profiling. Plant J. 88, 1058-1070.

Kwasnik, A., Wang, V.Y.-F., Krzyszton, M., Gozdek, A., Zakrzewska-Placzek, M., Stepniak, K., Poznanski, J., Tong, L., and Kufel, J. (2019). Arabidopsis DXO1 links RNA turnover and chloroplast function independently of its enzymatic activity. Nucleic Acids Res. 47, 4751-4764.

Li, F., Zheng, Q., Ryvkin, P., Dragomir, I., Desai, Y., Aiyer, S., Valladares, O., Yang, J., Bambina, S., Sabin, L.R., et al. (2012). Global analysis of RNA secondary structure in two metazoans. Cell Rep. 1, 69-82.

Liu, L., and Chen, X. (2016). RNA quality control as a key to suppressing RNA silencing of endogenous genes in plants. Mol. Plant 9, 826-836.

Love, M.I., Huber, W., and Anders, S. (2014). Moderated estimation of fold change and dispersion for RNA-seq data with DESeq2. Genome Biol. 15, 550.

Lyons, E., Pedersen, B., Kane, J., Alam, M., Ming, R., Tang, H., Wang, X., Bowers, J., Paterson, A., Lisch, D., and Freeling, M. (2008). Finding and comparing syntenic regions among Arabidopsis and the outgroups papaya, poplar, and grape: CoGe with Rosids. Plant Physiol. 148, 1772-1781.

Martin, M. (2011). Cutadapt removes adapter sequences from highthroughput sequencing reads. EMBnet J. 17, 10.

Martínez de Alba, A.E., Moreno, A.B., Gabriel, M., Mallory, A.C., Christ, A., Bounon, R., Balzergue, S., Aubourg, S., Gautheret, D., Crespi, M.D., et al. (2015). In plants, decapping prevents RDR6-dependent production of small interfering RNAs from endogenous mRNAs. Nucleic Acids Res. 43, 2902-2913

Nachtergaele, S., and He, C. (2017). The emerging biology of RNA post-transcriptional modifications. RNA Biol. 14, 156-163.

Pan, S., Li, K.E., Huang, W., Zhong, H., Wu, H., Wang, Y., Zhang, H., Cai, Z., Guo, H., Chen, X., and Xia, Y. (2020). Arabidopsis DXO1 possesses deNADding and exonuclease activities and its mutation affects defense-related and photosynthetic gene expression. J. Integr. Plant. Biol. 62, 967–983.

Peragine, A., Yoshikawa, M., Wu, G., Albrecht, H.L., and Poethig, R.S. (2004). SGS3 and SGS2/SDE1/RDR6 are required for juvenile development and the production of trans-acting siRNAs in Arabidopsis. Genes Dev. 18, 2368–2379.

Robinson, M.D., McCarthy, D.J., and Smyth, G.K. (2010). edgeR: a Bioconductor package for differential expression analysis of digital gene expression data. Bioinformatics 26, 139-140.

Silverman, I.M., Li, F., Alexander, A., Goff, L., Trapnell, C., Rinn, J.L., and Gregory, B.D. (2014). RNase-mediated protein footprint sequencing reveals protein-binding sites throughout the human transcriptome. Genome Biol.

Tamura, K., Peterson, D., Peterson, N., Stecher, G., Nei, M., and Kumar, S. (2011). MEGA5: molecular evolutionary genetics analysis using maximum likelihood, evolutionary distance, and maximum parsimony methods. Mol. Biol. Evol. 28, 2731-2739.

Thimm, O., Bläsing, O., Gibon, Y., Nagel, A., Meyer, S., Krüger, P., Selbig, J., Müller, L.A., Rhee, S.Y., and Stitt, M. (2004). mapman: a user-driven tool to display genomics data sets onto diagrams of metabolic pathways and other biological processes. Plant J. 37, 914-939.

Valkov, E., Muthukumar, S., Chang, C.T., Jonas, S., Weichenrieder, O., and Izaurralde, E. (2016). Structure of the Dcp2–Dcp1 mRNA-decapping complex in the activated conformation. Nat. Struct. Mol. Biol. 23, 574-579.

Vandivier, L.E., Campos, R., Kuksa, P.P., Silverman, I.M., Wang, L.S., and Gregory, B.D. (2015). Chemical modifications mark alternatively spliced and uncapped messenger RNAs in Arabidopsis. Plant Cell 27, 3024-3037.

Vvedenskaya, I.O., Bird, J.G., Zhang, Y., Zhang, Y., Jiao, X., Barvík, I., Krásný, L., Kiledjian, M., Taylor, D.M., Ebright, R.H., and Nickels, B.E. (2018). CapZyme-Seq comprehensively defines promoter-sequence determinants for RNA 5' capping with NAD+. Mol. Cell 70, 553-564.e9.

Walters, R.W., Matheny, T., Mizoue, L.S., Rao, B.S., Muhlrad, D., and Parker, R. (2017). Identification of NAD+ capped mRNAs in Saccharomyces cerevisiae. Proc. Natl. Acad. Sci. USA 114, 480-485.

Wang, Y., Li, S., Zhao, Y., You, C., Le, B., Gong, Z., Mo, B., Xia, Y., and Chen, X. (2019). NAD+-capped RNAs are widespread in the Arabidopsis transcriptome and can probably be translated. Proc. Natl. Acad. Sci. USA 116,

Wawer, I., Golisz, A., Sulkowska, A., Kawa, D., Kulik, A., and Kufel, J. (2018). mRNA decapping and 5'-3' decay contribute to the regulation of ABA signaling in Arabidopsis thaliana. Front. Plant Sci. 9, 312.

Willmann, M.R., Berkowitz, N.D., and Gregory, B.D. (2014). Improved genomewide mapping of uncapped and cleaved transcripts in eukaryotes-GMUCT 2.0. Methods 67, 64-73.

Willmann, M.R., Endres, M.W., Cook, R.T., and Gregory, B.D. (2011). The functions of RNA-dependent RNA polymerases in Arabidopsis. Arabidopsis Book 9. e0146.

Xiang, C., Han, P., Lutziger, I., Wang, K., and Oliver, D.J. (1999). A mini binary vector series for plant transformation. Plant Mol. Biol. 40, 711-717.

Xiang, S., Cooper-Morgan, A., Jiao, X., Kiledjian, M., Manley, J.L., and Tong, L. (2009). Structure and function of the $5' \rightarrow 3'$ exoribonuclease Rat1 and its activating partner rai1. Nature 458, 784-788.

Xiao, W., Wang, R.S., Handy, D.E., and Loscalzo, J. (2018). NAD(H) and NADP(H) redox couples and cellular energy metabolism. Antioxid. Redox Signal. 28, 251-272.

Yoshimura, K., and Shigeoka, S. (2015). Versatile physiological functions of the Nudix hydrolase family in Arabidopsis. Biosci. Biotechnol. Biochem. 79,

Yu, X., Willmann, M.R., Anderson, S.J., and Gregory, B.D. (2016). Genomewide mapping of uncapped and cleaved transcripts reveals a role for the





nuclear mRNA cap-binding complex in Cotranslational RNA decay in Arabidopsis. Plant Cell 28, 2385-2397.

Zhang, H., Zhong, H., Zhang, S., Shao, X., Ni, M., Cai, Z., Chen, X., and Xia, Y. (2019). NAD tagSeq reveals that NAD + -capped RNAs are mostly produced from a large number of protein-coding genes in Arabidopsis. Proc. Natl. Acad. Sci. USA 116, 12072-12077.

Zhang, X., and Guo, H. (2017). mRNA decay in plants: both quantity and quality matter. Curr. Opin. Plant Biol. 35, 138-144.

Zhang, X., Zhu, Y., Liu, X., Hong, X., Xu, Y., Zhu, P., Shen, Y., Wu, H., Ji, Y., Wen, X., et al. (2015). Plant biology. Suppression of endogenous gene silencing by bidirectional cytoplasmic RNA decay in Arabidopsis. Science 348, 120-123.

Zheng, Q., Ryvkin, P., Li, F., Dragomir, I., Valladares, O., Yang, J., Cao, K., Wang, L.S., and Gregory, B.D. (2010). Genome-wide double-stranded RNA sequencing reveals the functional significance of base-paired RNAs in Arabidopsis. PLoS Genet. 6, e1001141.

Developmental Cell Article



STAR*METHODS

KEY RESOURCES TABLE

REAGENT or RESOURCE	SOURCE	IDENTIFIER
Chemicals, Peptides, and Recombinant Proteins		
Abscisic acid (ABA)	Sigma-Aldrich	Cat#A4906
Na-HEPES	Sigma-Aldrich	Cat#H7006
ADP-ribosylcyclase (ADPRC)	Sigma-Aldrich	Cat#A9106-1VL
4-pentyn-1-ol	Sigma-Aldrich	Cat#302481
3-Nicotinamide adenine dinucleotide hydrate (NAD)	Sigma-Aldrich	Cat#N7004
CuSO ₄	Sigma-Aldrich	Cat#C1297
ГНРТА	Sigma-Aldrich	Cat#762342
Sodium ascorbate	Sigma-Aldrich	Cat#A7631
Biotin azide	Sigma-Aldrich	Cat#CLK-AZ104P4-25
Acetylated BSA	Sigma-Aldrich	Cat#B8894
K-Gluc (5-bromo-4-chloro-3-indolyl β-D-glucuronide)	Sigma-Aldrich	Cat#B5285
Sucrose	Sigma-Aldrich	Cat#S8501
Dynabeads MyOne Streptavidin C1	Thermo Fisher Sci.	Cat#65001
RNaseOUT	Thermo Fisher Sci.	Cat#LS10777019
Γ4 polynucleotide kinase	New England Biolabs	Cat#M0201S
Γ4 RNA ligase 1	New England Biolabs	Cat#M0204S
Γ4 RNA ligase 2, truncated	New England Biolabs	Cat#M0242S
10× NEB Buffer 2	New England Biolabs	Cat#B7002S
I0mM ATP	New England Biolabs	Cat#P0756S
Duplex Specific Nuclease (DSN)	Evrogen	Cat#EA001
50 mM dNTPs (12.5 mM of each)	Promega	Cat#U1420
Sodium Acetate (3 M), pH 5.5, RNase-free	Thermo Fisher Sci.	Cat#AM9740
Glycogen	Thermo Fisher Sci.	Cat#AM9510
Qiazol	Qiagen	Cat#79306
Chloroform:Isoamyl alcohol	Sigma-Aldrich	Cat#C0549
Phenol:chloroform	Sigma-Aldrich	Cat#77617
2-propanol	Sigma-Aldrich	Cat#34863
EDTA	Sigma-Aldrich	Cat#BP2483
100% ethanol	Decon Labs	Cat#2716
Jrea	Thermo Fisher Sci.	Cat#BP169
Tris-HCL	Thermo Fisher Sci.	Cat#15567-027
NaCl (5 M), RNase-free	Thermo Fisher Sci.	Cat#AM9759
Magnesium Chloride (MgCl2), 1 M Solution	Affymatrix	Cat#78641
Actinomycin D	Research Products International	Cat#A10025-0.005
Cordycepin	Sigma-Aldrich	Cat#C3394-25MG
Critical Commercial Assays		
Taql	New England Biolabs	Cat#Taql-v2
MEGAscript T7 Transcription Kit	Thermo Fisher Sci.	Cat#AM1334
Dynabeads mRNA DIRET Purification Kit	Thermo Fisher Sci.	Cat#61011
miRNeasy Mini Kit	Qiagen	Cat#217004
RNA Fragmentation Reagents	Thermo Fisher Sci.	Cat#AM8740
RNase-Free DNase Set	Qiagen	Cat#79254
SuperScript II Reverse Transcriptase	Thermo Fisher Sci.	Cat#18064014

(Continued on next page)





Developmental CellArticle

Continued		
REAGENT or RESOURCE	SOURCE	IDENTIFIER
Phusion High-Fidelity DNA Polymerase	New England Biolabs	Cat#M0531S
2x SYBR Green qPCR Master Mix	Bimake	Cat#B21202
Deposited Data		
Raw and processed NAD captureSeq (NADseq) data	This paper	GEO: GSE142390
Raw and processed polyA+-selected RNA sequencing (mRNA-seq) data	This paper	GEO: GSE142390
Raw and processed small RNA sequencing (smRNAseq) data	This paper	GEO: GSE142390
Raw and processed GMUCT data	This paper	GEO: GSE142390
Raw and processed GMUCT data (Col-0)	Willmann et al., 2014	GEO: GSE47121
EPIC-CoGe genome browser	Lyons and Freeling, 2008	https://genomevolution.org/coge/ NotebookView.pl?nid=2708
TAIR10 Arabidopsis annotation	TAIR	ftp://ftp.arabidopsis.org/home/tair/ Genes/ TAIR10_genome_release/
Experimental Models: Organisms/Strains		
Arabidopsis thaliana: Col-0	ABRC	CS70000
Arabidopsis thaliana: dxo1-1	ABRC	SALK_103157
Arabidopsis thaliana: dxo1-2	ABRC	SALK_032903
Arabidopsis thaliana: rdr6-11	Peragine et al., 2004	CS67869
Arabidopsis thaliana: rdr6-11 dxo1-2	This study	N/A
Arabidopsis thaliana: pDXO1::DXO1-GUS dxo1-2	This study	N/A
Arabidopsis thaliana: pUBQ10::DXO1-eGFP dxo1-2	This study	N/A
Oligonucleotides		
Oligo(dT) ₁₂₋₁₈ primers	Thermo Fisher Sci.	Cat#18418012
Genotyping primers	Table S8; this study	N/A
TruSeq adaptors, primers and indices	Illumina	TruSeq Small RNA Sample Prep Kit
TruSeq RA3 3'-adapter with random hexamer primer	Willmann et al., 2014	N/A
qPCR primers	Table S8; this study	N/A
Software and Algorithms		
cutadapt v1.9.1	Martin, 2011	https://cutadapt.readthedocs.io/en/ stable/installation.html
STAR v2.4.2a	Dobin et al., 2013	https://github.com/alexdobin/STAR
HTseq v0.6.0	Anders et al., 2015	https://github.com/simon-anders/htsed
DEseq2 v1.18.1	Love et al., 2014	https://bioconductor.org/biocLite.R
edgeR v3.26.6	Robinson et al., 2010	https://bioconductor.org/biocLite.R
DAVID online tool	Huang et al., 2009	https://david.ncifcrf.gov
MEGA v5.2	Tamura et al., 2011	https://www.megasoftware.net
Other		
MS salts	Phytotech	Cat#M524
Phytoblend	Caisson	Cat#PTP01

RESOURCE AVAILABILITY

Lead Contact

Further information and requests for resources and reagents should be directed to and will be fulfilled by the Lead Contact, Dr. Brian D. Gregory (bdgregor@sas.upenn.edu).

Materials Availability

All constructs and plant lines developed for this project are available upon request to the Lead Contact, Dr. Brian D. Gregory (bdgregor@sas.upenn.edu).

Article



Data and Code Availability

The raw and processed data for NAD-seq, total RNA-seq, GMUCT, polyA-selected (polyA) RNA-seq (mRNA-seq), and smRNA-seq libraries made with RNA extracted from unopened flower buds and 12-day-old seedlings (with and without 0.5 μ M ABA treatment) of Col-0 and dxo1 mutants as well as smRNA-seq libraries for rdr6-11 dxo1-2 unopened flower buds has been deposited in the NCBI Gene Expression Omnibus (http://www.ncbi.nlm.nih.gov/geo) database under the accession number GEO: GSE142390. Previously published GMUCT data for Col-0 unopened flower buds were obtained from GEO using the accession number GEO: GSE47121 (Willmann et al., 2014). The gene accession numbers for DXO1 and RDR6 are AT4G17620 and AT3G49500, respectively. The sequencing data presented here is also available through the EPIC-CoGe genome browser (Lyons et al., 2008): https://genomevolution.org/coge/NotebookView.pl?nid=2708.

EXPERIMENTAL MODEL AND SUBJECT DETAILS

Plant Materials

All plant lines used in this study were in the genetic background of *Arabidopsis thaliana* Columbia-0 (Col-0) ecotype. Plants of the Col-0 ecotype served as our wild-type plants in all experiments. Two T-DNA insertion alleles of the *DXO1* gene (*AT4G17620*) in the genetic background of *Arabidopsis thaliana* Columbia-0 (Col-0) ecotype from the Salk Insertional Mutant Collection were used in this study. One is SALK_103157 (*dxo1-1*) that has a T-DNA insertion in the second exon, and other is SALK_032903 (*dxo1-2*) which contains a T-DNA insertion in the fifth intron. *dxo1-2* was crossed with *rdr6-11* to obtain the double mutant *rdr6-11 dxo1-2*. The primers used for genotyping these various mutant lines are listed in Table S8. The genotyping for the *rdr6-11* mutation was performed by amplifying DNA samples with the primers listed in Table S8, and digesting the resulting PCR products with Taq1. Samples displaying two bands with lengths of 109 base pairs (bp) and 78 bp are *rdr6-11* homozygotes, samples showing two bands with lengths of 94 bp and 78 bp are wild-type plants, and samples showing all the three bands (109 bp, 94 bp and 78 bp), are heterozygotes (Peragine et al., 2004). All plants used in this study were grown in growth chambers under long days conditions (16 hours light and 8 hours dark photoperiod) at 22°C. For sampling unopened flower buds as well as phenotypic analyses of all genetic backgrounds, these plants were grown on soil. For sampling and analyzing 12-day-old seedlings with and without ABA treatment, these plants were grown vertically

on ½ Murashige and Skoog (MS) medium (Phytotech Labs, Lenexa, KS, USA) without and with varying concentrations of ABA.

Generation of pDXO1::DXO1-GUS::DXO1-3'UTR dxo1-2 Plants

pDXO1::DXO1-GUS::DXO1-3'UTR was made starting with a modified version of pCAMBIA3301 that had the p35S::BAR fragment replaced with pNOS::BAR which was amplified from pCB302 (Xiang et al., 1999), restricting the PCR fragment with BstXI and XhoI, and inserting it into pCAMBIA3301. The starting clone also had everything removed between EcoRI and BstEII and replaced with a DNA sequence that included EcoRI, StuI, RsrII, and BstEII sites, in that order. The DXO1 3' UTR was amplified from just downstream of the DXO1 stop codon to just before the start codon of the downstream gene (AT4G17640). This 592 bp product was restricted with RsrII and BstEII and inserted between those two sites of the vector. Then, the DXO1 promoter and coding region were amplified from CoI-0 genomic DNA, amplifying from immediately downstream of the upstream gene's (AT4G17616) stop codon through the coding region of AT4G17620 (DXO1) but not including the stop codon. The 3236 bp product was restricted to completion by StuI and partially with EcoRI because the 3236 bp product had an internal EcoRI site and was inserted between the EcoRI and StuI sites of the modified pCAMBIA3301 vector. Finally, GUS was amplified from pCAMBIA3301, restricted with StuI and RsrII, and inserted between those sites of the vector. The construct was transformed into dxo1-2 mutant plants through floral dip. All primers are listed in Table S8.

Generation of pUBQ10::DX01-eGFP dxo1-2 Plants

pUBQ10::DX01-eGFP was made starting with a modified version of pCAMBIA3301 that had the p35S::BAR fragment replaced with pNOS::BAR which was amplified from pCB302 (Xiang et al., 1999), restricting the PCR fragment with BstXI and XhoI, and inserting it into pCAMBIA3301. A pUBQ10-Spel-MCS-NcoI-UBQ10 3'UTR cassette was restricted from the pSY06 clone with HindIII and EcoRI and inserted between the HindIII and EcoRI sites of the modified version of pCAMBIA3301 vector. The resulting plasmid was then restricted with HindIII and BstEII, blunted, and ligated to remove p35S::GUS. The pUBQ10 was 636 bp and the 3'UTR was 382 bp. The DX01 CDS (but not including the stop codon) was amplified from cDNA of CoI-0, fully restricted with StuI (a site in the MCS) and partially with SpeI, and the 1644 bp product was inserted between the SpeI and StuI sites within the vector. eGFP was amplified from the vector HBT95 (Chiu et al., 1996) with primers specified in Table S8, restricted with StuI and NcoI, and inserted. The construct was transformed into dxo1-2 mutant plants through floral dip. All primers are listed in Table S8.

METHOD DETAILS

Histochemical Analysis of pDXO1::DXO1-GUS dxo1-2 Plants

For histochemical analysis of $pDXO1::DXO1-GUS\ dxo1-2$ plants, different tissues from multiple developmental stages were collected and stained with 5-bromo-4-chloro-3-indolyl β -D-glucuronide (X-gluc) (Sigma-Aldrich, St. Louis, MO, USA). To do this, the collected tissues were placed in 90% acetone for 15 minutes on ice, and then in X-Gluc buffer under vacuum for 16 hours at room temperature. After that, the samples were viewed via microscopy (Donnelly et al., 1999).





DXO1 Subcellular Localization Analysis Using pUBQ10::DXO1-eGFP/dxo1-2 Plants

To determine the subcellular localization of DXO1, Arabidopsis protoplasts and root tips of T2 pUBQ10::DXO1-eGFP dxo1-2 plants were analyzed using a fluorescent microscope.

Validation of NAD* Capture Approach Using In Vitro Luciferase Transcription

Luciferase transcripts (LUC) with NAD+ modification were in vitro transcribed using MEGAScript T7 Transcription Kit (ThermoFisher Scientific, Waltham, MA, USA) with the addition of the non-canonical nucleotide NAD+ (Sigma-Aldrich, St. Louis, MO, USA), while LUC transcribed without NAD+ was used as a negative control. We then performed NAD capture on these two populations of LUC transcripts as previously described (Cahová et al., 2015). Briefly, LUC with and without NAD+ addition was incubated with 4pentyn-1-ol (Sigma-Aldrich, St. Louis, MO, USA) with or without ADPRC (Sigma-Aldrich, St. Louis, MO, USA) at 37°C for 30 minutes. These reactions were then incubated with Copper-catalyzedazide-alkynecycloaddition (CuAAC) and biotin azide (Sigma-Aldrich, St. Louis, MO, USA) at 25°C for 30 minutes for to allow the click reaction to occur. Subsequently, Dynabeads MyOne Streptavidin C1 beads (ThermoFisher Scientific, Waltham, MA, USA) were used to pull down the biotinylated RNAs. Different to NAD captureSeq which immediately proceeds to on-bead ligation, reverse transcription of captured RNA, and release of cDNA from streptavidin beads by alkaline digest (Cahová et al., 2015), we added 10 mM EDTA (pH 8.2) and 95% formamide to elute biotinylated RNAs from the streptavidin beads, and eluted RNAs were purified by RNA precipitation with 100% EtOH (NAD-seg). Finally, reverse transcription was performed with gene specific primers (LUC specific primer) using SuperScript II (ThermoFisher Scientific, Waltham, MA, USA). Quantitative PCR (qPCR) was performed using SYBR Green 2X master mix (Bimake, Houston, TX, USA) to detect the LUC abundance in three biological replicates of each treatment condition using LUC specific primers described in Table S8. Significance between differences in detected LUC abundance between the various treatments was assessed using a Student's t test.

RNA Extraction

All experiments described in this study were performed with RNA extracted from unopened flower buds, 21-day-old seedlings, or 12day-old seedlings (as specified) homogenized using a liquid N2 cooled mortar and pestle. RNA was extracted from homogenate using Qiazol lysis reagent, and further homogenized using Qiashredders (Qiagen, Valencia, CA, USA). RNA was then isolated using Qiagen miRNEasy mini columns (Qiagen, Valencia, CA, USA), as described in the included protocol. All RNA was then treated with RNasefree DNase (Qiagen, Valencia, CA, USA) at room temperature for 30 minutes and subsequently ethanol precipitated.

In Vivo NAD-seq Library Construction

NAD+ RNA capture was performed by first DNase treating total RNA extracted from two biological replicates of unopened flower buds or 12-day-old seedlings with and with 0.5 µM ABA treatment of Col-0 and dxo1 mutants as described above for the LUC control experiments. The eluted biotinylated RNAs from these NAD+ RNA capture reactions were precipitated using 100% ethanol, and then fragmented using RNA Fragmentation Reagents (Thermo Fisher Scientific, Waltham, MA, USA). Subsequently, the fragmented RNA samples were treated with T4 polynucleotide kinase (New England Biolabs, Ipswich, MA, USA) to produce RNA fragments with 5' phosphates (5' P) and 3' OHs that are competent for subsequent RNA cloning steps necessary for sequencing library preparation. Sequencing library construction was then performed using the TruSeq Small RNA Sample Prep Kit using the included protocol (Illumina, San Diego, CA, USA) including adaptor ligation, reverse transcription, and PCR amplification with indexed primers as previously described (Zheng et al., 2010; Li et al., 2012; Silverman et al., 2014; Gosai et al., 2015). These sequencing libraries were then treated with Duplex Specific Nuclease (DSN) (Evrogen, Enzo Life Sciences, Farmingdale, NY, USA) to remove highly abundant RNA sequences as previously described (Silverman et al., 2014; Gosai et al., 2015). The resulting libraries were sequenced on an Illumina HiSeq2000 using the standard protocol for 50 base pair single-end sequencing.

Validation of NAD-seq by NAD-qPCR

Total RNA was extracted from three biological replicates of Col-0 and dxo1-2 unopened flower buds as described above. Subsequently, 1 nanogram of in vitro transcribed LUC RNA containing NAD+ modifications was spiked into 1 μg of total RNAs, and then each sample was divided into two parts evenly. Half was used as the total RNA background, while other half was used to perform NAD+ RNA capture as described above. Finally, reverse transcription was performed with random hexamers using SuperScript II (Thermo Fisher Scientific, Waltham, MA, USA). Quantification of transcript abundance by qRT-PCR was performed in NAD+ captured RNAs and total RNAs using SYBR Green 2X master mix (Bimake, Houston, TX, USA) following the manufacturer's protocol with primers listed in Table S8. LUC was used as a normalization control for the ΔΔCt analyses. Significance was assessed by Student's *t* test. Three biological replicates were used in these experiments.

polyA-selected and Total RNA-seq (mRNA- and RNA-seq) Library Construction

For mRNA-seq, two rounds of polyA+ selection was performed using Dynabeads mRNA DIRECT Purification Kit (Thermo Fisher Scientific, Waltham, MA, USA) on total RNA extracted from unopened flower buds or 12-day-old seedlings with and without 0.5 μM ABA treatment of Col-0 and dxo1-2 mutants. This polyA+ RNA was then used as the substrates in RNA-seq library construction as previously described (Anderson et al., 2018). Total RNA-seq library construction was performed similar to mRNA-seq with two exceptions: 1) polyA+ selection was omitted and 2) the sequencing libraries were subjected to a final DSN treatment (Evrogen, Enzo Life Sciences, Farmingdale, NY, USA) to remove highly abundant RNA sequences as previously described (Silverman et al., 2014; Gosai



Article



et al., 2015). The resulting libraries were sequenced on an Illumina HiSeq2000 using the standard protocol for 50-base pair single-end sequencing.

smRNA-seq Library Construction

Small RNA sequencing (smRNA-seq) libraries for unopened flower buds from Col-0, dxo1-2 single mutant, and rdr6-11 dxo1-2 double mutants were constructed using TruSeq Small RNA Sample Prep Kit using the included protocol (Illumina, San Diego, CA, USA). The resulting libraries were sequenced on an Illumina HiSeq2000 using the standard protocol for 50 base pair single-end sequencing.

Genome-wide Mapping of Uncapped and Cleaved Transcripts (GMUCT)

GMUCT libraries were constructed and sequenced for all samples described in this study (Col-0 and *dxo1* mutant unopened flower buds and 12-day-old seedlings with and without 0.5 μM ABA treatment) as previously described (Willmann et al., 2014). The resulting libraries were sequenced on an Illumina HiSeq2000 using the standard protocol for 50 base pair single-end sequencing.

Germination Test during ABA Treatment

Seeds of Col-0, dxo1-1, dxo1-2, and rdr6-11 dxo1-2 were plated on the ½ MS (Phytotech Labs, Lenexa, KS, USA) containing 1% sucrose and treated for 48 hours at 4°C. The plates were then transferred to 22°C and grown under long day conditions. To measure seed germination in response to ABA, the ½ MS (Phytotech Labs, Lenexa, KS, USA) media was supplemented with 0.2 μ M, 0.5 μ M, 2 μ M, or 10 μ M ABA (Sigma-Aldrich, St. Louis, MO, USA) dissolved in ethanol or ethanol alone that corresponded to the same concentration to act as a control (0 μ M), and the plates were incubated in a growth chamber horizontally (0.2 μ M, 0.5 μ M, and 2 μ M ABA) or vertically (0 and 10 μ M). After 7 days, the plates were photographed. These experiments were performed more than 3 times to act as multiple biological replicates. Representative images are shown in Figures 4A and S5A. To assess germination rate, seeds of Col-0, dxo1-2, and rdr6-11 dxo1-2 were sown on ½ MS without and with 0.5 μ M ABA and following a 48 hour at 4°C treatment they were grown vertically for 3 days. On day 4, the number of seeds that germinated, as measured by cotyledon emergence, was counted (n = 108 each genotype).

Liquid Chromatography-High Resolution Mass Spectrometry (LC-HRMS) to Detect Total NAD*

15-30 biological replicates of 21-day-old seedlings of Col-0, dxo1-2, and rdr6-11 dxo1-2 were used for detecting free NAD⁺. The seedlings for these genotypes were grown on ½ MS plates, harvested, and homogenized using a liquid N₂ cooled mortar and pestle. Total NAD⁺ was quantified in these powdered tissue samples using quantitative LC-HRMS with stable isotope labeled internal standards as previously described (Frederick et al., 2017).

qRT-PCR to Detect NAD* Biosynthesis Genes

Total RNA extracted from 21-day-old seedlings of Col-0, dxo1-2, and rdr6-11 dxo1-2 as described above was used as the substrate in reverse transcription reactions performed using oligo(dT) primers and SuperScript II (Thermo Fisher Scientific, Waltham, MA, USA). Quantification of transcript abundance (QPRT, NMNAT and NADS) by qRT-PCR was performed using SYBR Green 2X master mix (Bimake, Houston, TX, USA) following the manufacturer's protocol with primers listed in Table S8. ACT1 (AT2G37620) was used as an internal normalization control for the $\Delta\Delta$ Ct analyses. Significance was assessed by Student's t test. Three biological replicates were used in these experiments.

Transcript Stability Time Course

To measure mRNA stability, we first grew CoI-0 and dxo1-2 mutants seeds vertically on ½ MS (Phytotech Labs, Lenexa, KS, USA) media without or with 0.5 μ M ABA (Sigma-Aldrich, St. Louis, MO, USA) as described above. These control and ABA treated seedlings were carefully transferred into ½ MS (Phytotech Labs, Lenexa, KS, USA) liquid growth media containing 10 μ M Actinomycin D and 0.6 mM cordycepin (Sigma-Aldrich, St. Louis, MO, USA). Plants were then harvested at 0 and 24 hours post-treatment. Total RNA was extracted as described above and reverse transcribed using oligo dT primers (Thermo Fisher Scientific, Waltham, MA, USA). To measure the stability of NAD+ capped transcripts as compared to other transcripts from the same genes, total RNAs were performed using NAD+ capture (see description above), the NAD+ capped transcripts and other transcripts (supernatants) were purified and reverse transcribed using oligo dT (Thermo Fisher Scientific, Waltham, MA, USA). Quantification of total RNA abundance, NAD+ capped transcripts abundance and all other transcript populations from the same genes at 0 and 24 hours was performed using qRT-PCR with primers described in Table S8.

QUANTIFICATION AND STATISTICAL ANALYSIS

Identification of NAD* Capped RNAs

NAD-seq and RNA-seq reads were trimmed to remove the adapter sequences using cutadapt (v1.9.1) with default parameter (Martin, 2011). The trimmed reads were mapped to the Arabidopsis genome (TAIR10) using STAR (version 2.4.2a with "-outFilterMultimapN-max 10 -outFilterMismatchNoverLmax 0.10") (Dobin et al., 2013). Subsequently, read counts for each gene were calculated by htseq-count (HTseq v0.6.0) using the strand-specific parameters (Anders et al., 2015). Finally, negative binomial generalized linear models (DEseq2) (Love et al., 2014) were used to define significantly enriched NAD+ capped RNAs (false discovery rate < 0.1) in





NAD-seq samples as compared to total RNA-seq samples using the data from two independent biological replicates. All reads were normalized as reads per million (RPM). The NAD+ capped proportion metric was defined as the log₂ ratio of NAD+ capped reads of given transcripts as compared to total RNA-seq reads for the corresponding transcript (log₂[RPM_{NAD-seq}/RPM_{RNA-seq}]). The significant enrichment of gene ontology (GO) terms for the collections of NAD+ capped RNAs was performed with the gene ontology enrichment analysis using the DAVID tools set at default parameters (Huang et al., 2009).

Measurement of mRNA Stability Using the Proportion Uncapped Metric

RNA-seg and GMUCT raw reads (50 nt single-end sequences) were trimmed to remove the adapter sequences using cutadapt with default parameters (Martin, 2011). The trimmed reads were aligned to the Arabidopsis genome (TAIR10) using STAR as described above (Dobin et al., 2013). HTSeq was used to calculate the number of raw reads mapping to each given transcript using strand-specific parameters (Anders et al., 2015). The total mapping reads were normalized to reads per million (RPM). Proportion uncapped was defined as the log2 ratio of normalized GMUCT reads of a given transcript divided by the RNA-seq reads also to each corresponding transcript (log₂[RPM_{GMUCT}/RPM_{RNA-sed}]) for measuring the general level of RNA degradation as previously described (Anderson et al., 2018).

Differential Abundance Analysis

Gene counts for each transcript were called using HTseq-count on aligned RNA-seq reads using the parameters "-format=bam -stranded=reverse -mode=intersection-strict". Differentially abundant transcripts were identified using edgeR (v3.26.6) with the adjusted p-value < 0.05 (Robinson et al., 2010).

Small RNA Profiling

The smRNA-seq analyses were performed as previously described (Yu et al., 2016). Briefly, all small RNA reads (50 nt single-end sequences) were trimmed to remove the adapter sequences using cutadapt with default parameters (Martin, 2011). The trimmed reads were aligned to all full-length mature mRNAs found in the annotated Arabidopsis genome (TAIR10) using STAR as described above (Dobin et al., 2013). The perfect matching reads mapping to mature mRNAs were extracted and the length distribution of small RNA reads from 20-24 nt were counted in a strand-specific manner. The 21-22 nt small RNAs from both strands of each endogenous mRNA were counted. The edgeR (v3.26.6) (Robinson et al., 2010) analysis package was then used to define mRNAs producing significantly differentially abundant smRNAs between Col-0 and dxo1 mutant plants with an adjusted p value < 0.05.

Determination of Library Reproducibility

Read coverage of Arabidopsis transcripts were calculated and normalized using HTseq followed by DESeq2 analysis (Anders et al., 2015; Love et al., 2014) to perform distance measurement and principal component analysis for clustering the samples based on the normalized read counts of Arabidopsis transcripts.

Construction of a DXO1 Phylogenetic Tree

The protein sequences of DXO1 in 19 representative species including yeast, C. elegans, Drosophila, mouse, human, and Arabidopsis were downloaded through HomoloGene in NCBI. The multiple alignment of these protein sequences was performed using default parameters of the Molecular Evolutionary Genetics Analysis (MEGA) v5.2 software, and neighbor-joining trees were constructed using MEGA v5.2 (Tamura et al., 2011). The statistical strengths were assessed by bootstraps with 10,000 replicates.